Fraunhofer
ITWM

W. Arne, N. Marheineke, J. Schnebele, R. Wegener

Fluid-fiber-interactions in rotational spinning process of glass wool production

Berichte des Fraunhofer ITWM, Nr. 197 (2010)

ISSN 1434-9973

Bericht 197 (2010)

Die Veröffentlichungen in der Berichtsreihe des Fraunhofer ITWM können bezogen werden über:

Fraunhofer-Institut für Techno- und
Wirtschaftsmathematik ITWM
Fraunhofer-Platz 1

67663 Kaiserslautern
Germany

Telefon: +49(0)631/3160 0-0
Telefax: +49(0)631/3160 0-1099
E-Mail: info@itwm.fraunhofer.de
Internet: www.itwm.fraunhofer.de

Vorwort

Das Tätigkeitsfeld des Fraunhofer-Instituts für Techno- und Wirtschaftsmathematik ITWM umfasst anwendungsnahe Grundlagenforschung, angewandte Forschung sowie Beratung und kundenspezifische Lösungen auf allen Gebieten, die für Techno- und Wirtschaftsmathematik bedeutsam sind.

In der Reihe »Berichte des Fraunhofer ITWM« soll die Arbeit des Instituts kontinuierlich einer interessierten Öffentlichkeit in Industrie, Wirtschaft und Wissenschaft vorgestellt werden. Durch die enge Verzahnung mit dem Fachbereich Mathematik der Universität Kaiserslautern sowie durch zahlreiche Kooperationen mit internationalen Institutionen und Hochschulen in den Bereichen Ausbildung und Forschung ist ein großes Potenzial für Forschungsberichte vorhanden. In die Berichtreihe werden sowohl hervorragende Diplom- und Projektarbeiten und Dissertationen als auch Forschungsberichte der Institutsmitarbeiter und Institutsgäste zu aktuellen Fragen der Techno- und Wirtschaftsmathematik aufgenommen.

Darüber hinaus bietet die Reihe ein Forum für die Berichterstattung über die zahlreichen Kooperationsprojekte des Instituts mit Partnern aus Industrie und Wirtschaft.

Berichterstattung heißt hier Dokumentation des Transfers aktueller Ergebnisse aus mathematischer Forschungs- und Entwicklungsarbeit in industrielle Anwendungen und Softwareprodukte – und umgekehrt, denn Probleme der Praxis generieren neue interessante mathematische Fragestellungen.

Prof. Dr. Dieter Prätzel-Wolters
Institutsleiter

Kaiserslautern, im Juni 2001

Fluid-fiber-interactions in rotational spinning process of glass wool production

Walter Arne[1,2], Nicole Marheineke[3], Johannes Schnebele[2] and Raimund Wegener*[2]

[1]Universität Kassel, Fachbereich Mathematik und Naturwissenschaften, Heinrich Plett Str. 40, D-34132 Kassel, Germany
[2]Fraunhofer Institut für Techno- und Wirtschaftsmathematik (ITWM), Fraunhofer Platz 1, D-67663 Kaiserslautern, Germany
[3]FAU Erlangen-Nürnberg, Lehrstuhl Angewandte Mathematik 1, Martensstr. 3, D-91058 Erlangen, Germany

Email: W. Arne - arne@mathematik.uni-kassel.de; N. Marheineke - nicole.marheineke@am.uni-erlangen.de; J. Schnebele - johannes.schnebele@itwm.fraunhofer.de; R. Wegener - raimund.wegener@itwm.fraunhofer.de;

*Corresponding author

Abstract

The optimal design of rotational production processes for glass wool manufacturing poses severe computational challenges to mathematicians, natural scientists and engineers. In this paper we focus exclusively on the spinning regime where thousands of viscous thermal glass jets are formed by fast air streams. Homogeneity and slenderness of the spun fibers are the quality features of the final fabric. Their prediction requires the computation of the fluid-fiber-interactions which involves the solving of a complex three-dimensional multiphase problem with appropriate interface conditions. But this is practically impossible due to the needed high resolution and adaptive grid refinement. Therefore, we propose an asymptotic coupling concept. Treating the glass jets as viscous thermal Cosserat rods, we tackle the multiscale problem by help of momentum (drag) and heat exchange models that are derived on basis of slender-body theory and homogenization. A weak iterative coupling algorithm that is based on the combination of commercial software and self-implemented code for flow and rod solvers, respectively, makes then the simulation of the industrial process possible. For the boundary value problem of the rod we particularly suggest an adapted collocation-continuation method. Consequently, this work establishes a promising basis for future optimization strategies.

Keywords: Rotational spinning process, viscous thermal jets, fluid-fiber interactions, two-way coupling, slender-body theory, Cosserat rods, drag models, boundary value problem, continuation method

MSC-Classification. 76-xx, 34B08, 41A60, 65L10, 65Z05

1 Introduction

Glass wool manufacturing requires a rigorous understanding of the rotational spinning of viscous thermal jets exposed to aerodynamic forces. Rotational spinning processes consist in general of two regimes: melting and spinning. The plant of our industrial partner, Woltz GmbH in Wertheim, is illustrated in Figure 1. Glass is heated upto temperatures of 1050°C in a stove from which the melt is led to a centrifugal disk. The

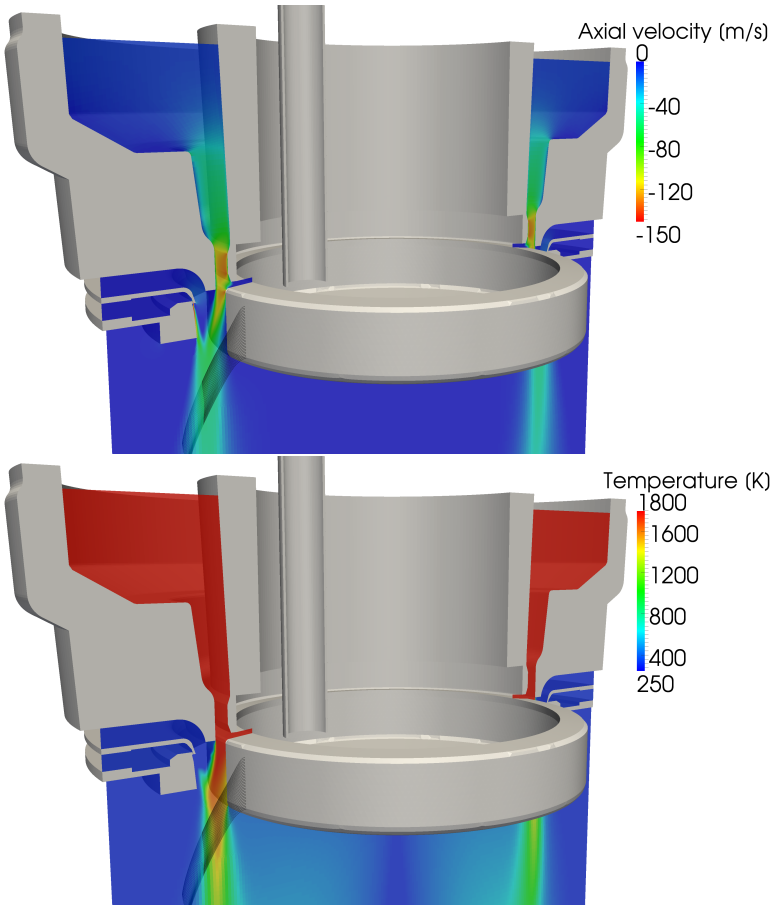

Figure 1: Rotational spinning process of the company Woltz GmbH. Sketch of set-up, some glass jets are exemplarily plotted as black curves. The color maps visualize axial velocity and temperature of the air flow, respectively.

walls of the disk are perforated by 35 rows over height with 770 equidistantly placed small holes per row. Emerging from the rotating disk via continuous extrusion, the liquid jets grow and move due to viscosity, surface tension, gravity and aerodynamic forces. There are in particular two different air flows that interact with the arising glass fiber curtain: a downwards-directed hot burner flow of 1500°C that keeps the jets near the nozzles warm and thus extremely viscous and shapeable as well as a highly turbulent cross-stream of 30°C that stretches and finally cools them down such that the glass fibers become hardened. Laying down onto a conveyor belt they yield the basic fabric for the final glass wool product. For the quality assessment of the fabrics the properties of the single spun fibers, i.e. homogeneity and slenderness, play an important role. A long-term objective in industry is the optimal design of the manufacturing process with respect to desired product specifications and low production costs. Therefore, it is necessary to model, simulate and control the whole process.

Up to now, the numerical simulation of the whole manufacturing process is impossible because of its enormous complexity. In fact, we do not long for an uniform numerical treatment of the whole process, but have the idea to derive adequate models and methods for the separate regimes and couple them appropriately, for a similar strategy for technical textiles manufacturing see [1]. In this content, the melting regime dealing with the creeping highly viscous melt flow from the stove to the holes of the centrifugal disk might be certainly

	Temperature		Velocity			Diameter		
Burner air flow in channel	T_{air1}	1773 K	V_{air1}	$1.2 \cdot 10^2$	m/s	W_1	$1.0 \cdot 10^{-2}$	m
Turbulent air stream at injector	T_{air2}	303 K	V_{air2}	$3.0 \cdot 10^2$	m/s	W_2	$2.0 \cdot 10^{-4}$	m
Centrifugal disk	T_{melt}	1323 K	Ω	$2.3 \cdot 10^2$	1/s	$2R$	$4.0 \cdot 10^{-1}$	m
Glass jets at spinning holes	θ	1323 K	U	$6.7 \cdot 10^{-3}$	m/s	D	$7.4 \cdot 10^{-4}$	m

Table 1: Typical temperature, velocity and length values in the considered rotational spinning process, Figure 1. There are $M = 35$ spinning rows, each with $N = 770$ nozzles. The resulting 26950 glass jets are stretched by a factor 10000 within the process, their slenderness ratio is $\delta \approx 10^{-4}$.

handled by standard models and methods from the field of fluid dynamics. It yields the information about the melt velocity and temperature distribution at the nozzles which is of main importance for the ongoing spinning regime. However, be aware that for their determination not only the melt behavior in the centrifugal disk but also the effect of the burner flow, i.e. aerodynamic heating and heat distortion of disk walls and nozzles, have to be taken into account. In this paper we assume the conditions at the nozzles to be given and focus exclusively on the spinning regime which is the challenging core of the problem. For an overview of the specific temperature, velocity and length values we refer to Table 1. In the spinning regime the liquid viscous glass jets are formed, in particular they are stretched by a factor 10000. Their geometry is characterized by a typical slenderness ratio $\delta = d/l \approx 10^{-4}$ of jet diameter d and length l. The resulting fiber properties (characteristics) depend essentially on the jets behavior in the surrounding air flow. To predict them, the interactions, i.e. momentum and energy exchange, of air flow and fiber curtain consisting of MN single jets ($M = 35$, $N = 770$) have to be considered. Their computation requires in principle a coupling of fiber jets and flow with appropriate interface conditions. However, the needed high resolution and adaptive grid refinement make the direct numerical simulation of the three-dimensional multiphase problem for ten thousands of slender glass jets and fast air streams not only extremely costly and complex, but also practically impossible. Therefore, we tackle the multiscale problem by help of drag models that are derived on basis of slender-body theory and homogenization, and a weak iterative coupling algorithm.

The dynamics of curved viscous inertial jets is of interest in many industrial applications (apart from glass wool manufacturing), e.g. in nonwoven production [1, 2], pellet manufacturing [3, 4] or jet ink design, and has been subject of numerous theoretical, numerical and experimental investigations, see [5] and references within. In the terminology of [6], there are two classes of asymptotic one-dimensional models for a jet, i.e. string and rod models. Whereas the string models consist of balance equations for mass and linear momentum, the more complex rod models contain also an angular momentum balance, [7, 8]. A string model for the jet dynamics was derived in a slender-body asymptotics from the three-dimensional free boundary value problem given by the incompressible Navier-Stokes equations in [5]. Accounting for inner viscous transport, surface tension and placing no restrictions on either the motion or the shape of the jet's center-line, it generalizes the previously developed string models for straight [9–11] and curved [12–14] center-lines. However, already in the stationary case the applicability of the string model turns out to be restricted to certain parameter ranges [15, 16] because of a non-removable singularity that comes from the deduced boundary conditions. These limitations can be overcome by a modification of the boundary conditions, i.e. the release of the condition for the jet tangent at the nozzle in favor of an appropriate interface condition, [17–19]. This involves two string models that exclusively differ in the closure conditions. For gravitational spinning scenarios they cover the whole parameter range, but in the presence of rotations there exist small parameter regimes where none of them works. A rod model that allows for stretching, bending and twisting was proposed and analyzed in [20, 21] for the coiling of a viscous jet falling on a rigid substrate. Based on these studies and embedded in the special Cosserat theory a modified incompressible isothermal rod model for rotational spinning was developed and investigated in [16,19]. It allows for simulations in the whole (Re, Rb, Fr)-range and shows its superiority to the string models. These observations correspond to studies on a fluid-mechanical "sewing machine", [22, 23]. By containing the slenderness parameter δ explicitely in the angular momentum balance, the rod model is no asymptotic model of zeroth order. Since its solutions

converge to the respective string solutions in the slenderness limit $\delta \to 0$, it can be considered as δ-regularized model, [19]. In this paper we extend the rod model by incorporating the practically relevant temperature dependencies and aerodynamic forces. Thereby, we use the air drag model F of [24] that combines Oseen and Stokes theory [25–27], Taylor heuristic [28] and numerical simulations. Being validated with experimental data [29–32], it is applicable for all air flow regimes and incident flow directions. Transferring this strategy, we model a similar aerodynamic heat source for the jet that is based on the Nusselt number Nu [33]. Our coupling between glass jets and air flow follows then the principle that action equals reaction. By inserting the corresponding homogenized source terms induced by F and Nu in the balance equations of the air flow, we make the proper momentum and energy exchange within this slender-body framework possible.

The paper is structured as follows. In Section 2 we start with the general coupling concept for slender bodies and fluid flows. Therefore, we introduce the viscous thermal Cosserat rod system and the compressible Navier-Stokes equations for glass jets and air flow, respectively, and present the models for the momentum and energy exchange: drag F and Nusselt function Nu. The special set-up of the industrial rotational spinning process allows for the simplification of the model framework, i.e. transition to stationarity and assumption of rotational invariance as we discuss in Section 3. Section 4 deals then with the numerical treatment. To realize the fiber-flow interactions we use a weak iterative coupling algorithm, which is adequate for the problem and has the advantage that we can combine commercial software and self-implemented code. Special attention is paid to the collocation and continuation method for solving the boundary value problem of the rod. The convergence of the coupling algorithm and simulation results for a specific spinning adjustment are shown in Section 5. This illustrates the applicability of our coupling framework as one of the basic tools for the optimal design of the whole manufacturing process. We conclude with some remarks to the process in Section 6.

2 General coupling concept for slender bodies and fluid flows

We are interested in the spinning of ten thousands of slender glass jets by fast air streams, $MN = 26950$. The glass jets form a kind of curtain that interact and crucially affect the surrounding air. The determination of the fluid-fiber-interactions requires in principle the simulation of the three-dimensional multiphase problem with appropriate interface conditions. However, regarding the complexity and enormous computational effort, this is practically impossible. Therefore, we propose a coupling concept for slender bodies and fluid flows that is based on drag force and heat exchange models. In this section we first present the two-way coupling of a single viscous thermal Cosserat rod and the compressible Navier-Stokes equations and then generalize the concept to many rods. Thereby, we choose an invariant formulation in the three-dimensional Euclidian space $\mathbb{E}^3$.

Note that we mark all quantities associated to the air flow by the subscript $_\star$ throughout the paper. Moreover, to facilitate the readability of the coupling concept, we introduce the abbreviations $\mathbf{\Psi}$ and $\mathbf{\Psi}_\star$ that represent all quantities of the glass jets and the air flow, respectively.

2.1 Models for glass jets and air flows

2.1.1 Cosserat rod

A glass jet is a slender body, i.e. a rod in the context of three-dimensional continuum mechanics. Because of its slender geometry, its dynamics might be reduced to a one-dimensional description by averaging the underlying balance laws over its cross-sections. This procedure is based on the assumption that the displacement field in each cross-section can be expressed in terms of a finite number of vector- and tensor-valued quantities. In the special Cosserat rod theory, there are only two constitutive elements: a curve specifying the position $\mathbf{r} : Q \to \mathbb{E}^3$ and an orthonormal director triad $\{\mathbf{d_1}, \mathbf{d_2}, \mathbf{d_3}\} : Q \to \mathbb{E}^3$ characterizing the orientation of the cross-sections, where $Q = \{(s,t) \in \mathbb{R}^2 | s \in I(t) = [0, l(t)], t > 0\}$ with arclength parameter s and time t. For more details on the Cosserat theory see [6]. In the following we use an incompressible viscous Cosserat rod model that was derived on basis of the work [20, 34] on viscous rope coiling and investigated for isothermal curved

inertial jets in rotational spinning processes [16, 19]. We extend the model by incorporating temperature effects and aerodynamic forces. The rod system describes the variables of jet curve $\mathbf{r}$, orthonormal triad $\{\mathbf{d_1}, \mathbf{d_2}, \mathbf{d_3}\}$, generalized curvature $\boldsymbol{\kappa}$, convective speed u, cross-section A, linear velocity $\mathbf{v}$, angular velocity $\boldsymbol{\omega}$, temperature T and normal contact forces $\mathbf{n} \cdot \mathbf{d}_\alpha$, $\alpha = 1, 2$. It consists of four kinematic and four dynamic equations, i.e. balance laws for mass (cross-section), linear and angular momentum and temperature,

$$\begin{aligned} \partial_t \mathbf{r} &= \mathbf{v} - u\mathbf{d_3} \\ \partial_t \mathbf{d_i} &= (\boldsymbol{\omega} - u\boldsymbol{\kappa}) \times \mathbf{d_i} \\ \partial_s \mathbf{r} &= \mathbf{d_3} \\ \partial_s \mathbf{d_i} &= \boldsymbol{\kappa} \times \mathbf{d_i} \\ \partial_t A + \partial_s(uA) &= 0 \\ \rho\left(\partial_t(A\mathbf{v}) + \partial_s(uA\mathbf{v})\right) &= \partial_s \mathbf{n} + \rho A g \mathbf{e_g} + \mathbf{f}_{air} \\ \rho\left(\partial_t(\mathbf{J}\cdot\boldsymbol{\omega}) + \partial_s(u\mathbf{J}\cdot\boldsymbol{\omega})\right) &= \partial_s \mathbf{m} + \mathbf{d_3} \times \mathbf{n} \\ \rho c_p\left(\partial_t(AT) + \partial_s(uAT)\right) &= q_{rad} + q_{air} \end{aligned} \tag{1}$$

supplemented with an incompressible geometrical model of circular cross-sections with diameter d

$$\mathbf{J} = I(\mathbf{d_1} \otimes \mathbf{d_1} + \mathbf{d_2} \otimes \mathbf{d_2} + 2\mathbf{d_3} \otimes \mathbf{d_3}), \qquad I = \frac{\pi}{64} d^4, \qquad A = \frac{\pi}{4} d^2$$

as well as viscous material laws for the tangential contact force $\mathbf{n} \cdot \mathbf{d_3}$ and contact couple $\mathbf{m}$

$$\mathbf{n} \cdot \mathbf{d_3} = 3\mu A \partial_s u, \qquad \mathbf{m} = 3\mu I \left(\mathbf{d_1} \otimes \mathbf{d_1} + \mathbf{d_2} \otimes \mathbf{d_2} + \frac{2}{3}\mathbf{d_3} \otimes \mathbf{d_3}\right) \cdot \partial_s \boldsymbol{\omega}.$$

Rod density ρ and heat capacity c_p are assumed to be constant. The temperature-dependent dynamic viscosity μ is modeled according to the Vogel-Fulcher-Tamman relation[1]. The external loads rise from gravity $\rho A g \mathbf{e_g}$ with gravitational acceleration g and aerodynamic forces $\mathbf{f}_{air}$. In the temperature equation we neglect inner friction and heat conduction and focus exclusively on radiation q_{rad} and aerodynamic heat sources q_{air}. The radiation effect depends on the geometry of the plant and is incorporated in the system by help of the simple model

$$q_{rad} = \varepsilon_R \sigma \pi d (T_{ref}^4 - T^4)$$

with emissivity ε_R, Stefan-Boltzmann constant σ and reference temperature T_{ref}. Appropriate initial and boundary conditions close the rod system.

2.1.2 Navier-Stokes equations

A compressible air flow in the space-time domain $\Omega_t = \{(\mathbf{x}, t) | \mathbf{x} \in \Omega \subset \mathbb{E}^3, t > 0\}$ is described by density $\rho_\star$, velocity $\mathbf{v}_\star$, temperature $T_\star$. Its model equations consist of the balance laws for mass, momentum and energy,

$$\begin{aligned} \partial_t \rho_\star + \nabla \cdot (\mathbf{v}_\star \rho_\star) &= 0 \\ \partial_t(\rho_\star \mathbf{v}_\star) + \nabla \cdot (\mathbf{v}_\star \otimes \rho_\star \mathbf{v}_\star) &= \nabla \cdot \mathbf{S}_\star^T + \rho_\star g \mathbf{e_g} + \mathbf{f}_{jets} \\ \partial_t(\rho_\star e_\star) + \nabla \cdot (\mathbf{v}_\star \rho_\star e_\star) &= \mathbf{S}_\star : \nabla \mathbf{v}_\star - \nabla \cdot \mathbf{q}_\star + q_{jets} \end{aligned} \tag{2}$$

supplemented with the Newtonian stress tensor $\mathbf{S}_\star$, the Fourier law for heat conduction $\mathbf{q}_\star$

$$\mathbf{S}_\star = -p_\star \mathbf{I} + \mu_\star(\nabla \mathbf{v}_\star + \nabla \mathbf{v}_\star^T) + \lambda_\star \nabla \cdot \mathbf{v}_\star \mathbf{I}, \qquad \mathbf{q}_\star = -k_\star \nabla T_\star,$$

[1] The Vogel-Fulcher-Tamman relation for the temperature-dependent viscosity reads $\mu(T) = 10^{p_1 + p_2/(T - p_3)}$ Pa s where we use the parameters $p_1 = -2.56$, $p_2 = 4289.18$ K and $p_3 = (150.74 + 273.15)$ K, [33].

as well as thermal and caloric equations of state of a ideal gas

$$p_\star = \rho_\star R_\star T_\star, \qquad e_\star = \int_0^{T_\star} c_{p\star}(T)\mathrm{d}T - \frac{p_\star}{\rho_\star}$$

with pressure $p_\star$ and inner energy $e_\star$. The specific gas constant for air is denoted by $R_\star$. The temperature-dependent viscosities $\mu_\star$, $\lambda_\star$, heat capacity $c_{p\star}$ and heat conductivity $k_\star$ can be modeled by standard polynomial laws, see e.g. [33, 35]. External loads rise from gravity $\rho_\star g\mathbf{e_g}$ and forces due to the immersed fiber jets $\mathbf{f}_{jets}$. These fiber jets also imply a heat source q_{jets} in the energy equation. Appropriate initial and boundary conditions close the system.

2.2 Models for momentum and energy exchange

The coupling of the Cosserat rod and the Navier-Stokes equations is performed by help of drag forces and heat sources. Taking into account the conservation of momentum and energy, $\mathbf{f}_{air}$ and $\mathbf{f}_{jets}$ as well as q_{air} and q_{jets} satisfy the principle that action equals reaction and obey common underlying relations. Hence, we can handle the delicate fluid-fiber-interactions by help of two surrogate models, so-called exchange functions, i.e. a dimensionless drag force F (inducing $\mathbf{f}_{air}$, $\mathbf{f}_{jets}$) and Nusselt number Nu (inducing q_{air}, q_{jets}). For a flow around a slender long cylinder with circular cross-sections there exist plenty of theoretical, numerical and experimental investigations to these relations in literature, for an overview see [24] as well as e.g. [29,30,33,36] and references within. We use this knowledge locally and globalize the models by superposition to apply them to our curved moving Cosserat rod. This strategy follows a Global-from-Local concept [37] that turned out to be very satisfying in the derivation and validation of a stochastic drag force in a one-way coupling of fibers in turbulent flows [24].

2.2.1 *Drag forces – $\mathbf{f}_{air}$ vs. $\mathbf{f}_{jets}$*

Let $\mathbf{\Psi}$ and $\mathbf{\Psi}_\star$ represent all glass jet and air flow quantities, respectively. Then, the drag forces are given by

$$\mathbf{f}_{air}(s,t) = \boldsymbol{\mathcal{F}}(\mathbf{\Psi}(s,t), \mathbf{\Psi}_\star(\mathbf{r}(s,t),t)), \qquad \mathbf{f}_{jets}(\mathbf{x},t) = -\int_{I(t)} \delta(\mathbf{x}-\mathbf{r}(s,t))\, \boldsymbol{\mathcal{F}}(\mathbf{\Psi}(s,t), \mathbf{\Psi}_\star(\mathbf{x},t))\,\mathrm{d}s$$

$$\boldsymbol{\mathcal{F}}(\mathbf{\Psi}, \mathbf{\Psi}_\star) = \frac{\mu_\star^2}{d\rho_\star}\, \boldsymbol{F}(\mathbf{d_3}, \frac{d\rho_\star}{\mu_\star}(\mathbf{v}_\star - \mathbf{v}))$$

where δ the Dirac distribution. By construction, they fulfill the principle that action equals reaction and hence the momentum is conserved, i.e.

$$\int_{I_V(t)} \mathbf{f}_{air}(s,t)\,\mathrm{d}s = -\int_V \mathbf{f}_{jets}(\mathbf{x},t)\,\mathrm{d}\mathbf{x}$$

for an arbitrary domain V and $I_V(t) = \{s \in I(t) | \mathbf{r}(s,t) \in V(t)\}$. The (line) force $\boldsymbol{\mathcal{F}}$ acting on a slender body is caused by friction and inertia. It depends on material and geometrical properties as well as on the specific inflow situation. The number of dependencies can be reduced to two by help of non-dimensionalizing which yields the dimensionless drag force $\boldsymbol{F}$ in dependence on the jet orientation (tangent) and the dimensionless relative velocity between air flow and glass jet. Due to the rotational invariance of the force, the function

$$\boldsymbol{F} : S^2 \times \mathbb{E}^3 \to \mathbb{E}^3$$

can be associated with its component tupel F for every representation in an orthonormal basis, i.e.

$$\mathrm{F} : S^2_{\mathbb{R}^3} \times \mathbb{R}^3 \to \mathbb{R}^3,$$

$$\mathrm{F} = (F_1, F_2, F_3) \quad \text{with} \quad \sum_{i=1}^{3} F_i(\tau, \mathsf{w})\mathbf{e_i} = \boldsymbol{F}\left(\sum_{i=1}^{3} \tau_i \mathbf{e_i}, \sum_{i=1}^{3} w_i \mathbf{e_i}\right) \text{ for every orthonormal basis } \{\mathbf{e_i}\}.$$

For F we use the drag model [24] that was developed on top of Oseen and Stokes theory [25–27], Taylor heuristic [28] and numerical simulations and validated with measurements [29–32]. It shows to be applicable for all air flow regimes and incident flow directions. Let $\{\mathbf{n}, \mathbf{b}, \boldsymbol{\tau}\}$ be the orthonormal basis induced by the specific inflow situation $(\boldsymbol{\tau}, \mathbf{w})$ with orientation $\boldsymbol{\tau}$ and velocity $\mathbf{w}$, assuming $\mathbf{w} \not\parallel \boldsymbol{\tau}$,

$$\mathbf{n} = \frac{\mathbf{w} - w_\tau \boldsymbol{\tau}}{w_n}, \qquad \mathbf{b} = \boldsymbol{\tau} \times \mathbf{n}, \qquad\qquad w_\tau = \mathbf{w} \cdot \boldsymbol{\tau}, \qquad w_n = \sqrt{\mathbf{w}^2 - w_\tau^2}.$$

Then, the force is given by

$$\boldsymbol{F}(\boldsymbol{\tau}, \mathbf{w}) = F_n(w_n)\mathbf{n} + F_\tau(w_n, w_\tau)\boldsymbol{\tau} \tag{3}$$
$$F_n(w_n) = w_n^2\, c_n(w_n) = w_n\, r_n(w_n), \qquad F_\tau(w_n, w_\tau) = w_\tau\, w_n\, c_\tau(w_n) = w_\tau\, r_\tau(w_n).$$

according to the Independence Principle [38]. The differentiable normal and tangential drag functions c_n, c_τ are

$$c_n(w_n) = \begin{cases} 4\pi/(S w_n)\,[1 - w_n^2(S^2 - S/2 + 5/16)/(32S)] & w_n < w_1 \\ \exp(\sum_{j=0}^{3} p_{n,j} \ln^j w_n) & w_1 \le w_n \le w_2 \\ 2/\sqrt{w_n} + 0.5 & w_2 < w_n \end{cases}$$
$$c_\tau(w_n) = \begin{cases} 4\pi/((2S-1) w_n)\,[1 - w_n^2(2S^2 - 2S + 1)/(16(2S-1))] & w_n < w_1 \\ \exp(\sum_{j=0}^{3} p_{\tau,j} \ln^j w_n) & w_1 \le w_n \le w_2 \\ \gamma/\sqrt{w_n} & w_2 < w_n \end{cases}$$

with $S(w_n) = 2.0022 - \ln w_n$, transition points $w_1 = 0.1$, $w_2 = 100$, amplitude $\gamma = 2$. The regularity involves the parameters $p_{n,0} = 1.6911$, $p_{n,1} = -6.7222 \cdot 10^{-1}$, $p_{n,2} = 3.3287 \cdot 10^{-2}$, $p_{n,3} = 3.5015 \cdot 10^{-3}$ and $p_{\tau,0} = 1.1552$, $p_{\tau,1} = -6.8479 \cdot 10^{-1}$, $p_{\tau,2} = 1.4884 \cdot 10^{-2}$, $p_{\tau,3} = 7.4966 \cdot 10^{-4}$. To be also applicable in the special case of a transversal incident flow $\mathbf{w} \parallel \boldsymbol{\tau}$ and to ensure a realistic smooth force $\boldsymbol{F}$, the drag is modified for $w_n \to 0$. A regularization based on the slenderness parameter δ matches the associated resistance functions r_n, r_τ (3) to Stokes resistance coefficients of higher order for $w_n \ll 1$, for details see [24].

2.2.2 *Heat sources – q_{air} vs. q_{jets}*

Analogously to the drag forces, the heat sources are given by

$$q_{air}(s,t) = \mathcal{Q}(\boldsymbol{\Psi}(s,t), \boldsymbol{\Psi}_\star(\mathbf{r}(s,t),t)), \qquad q_{jets}(\mathbf{x},t) = -\int_{I(t)} \delta(\mathbf{x} - \mathbf{r}(s,t))\, \mathcal{Q}(\boldsymbol{\Psi}(s,t), \boldsymbol{\Psi}_\star(\mathbf{x},t))\, \mathrm{d}s$$
$$\mathcal{Q}(\boldsymbol{\Psi}, \boldsymbol{\Psi}_\star) = 2k_\star\, \mathrm{Nu}\left(\frac{\mathbf{v}_\star - \mathbf{v}}{\|\mathbf{v}_\star - \mathbf{v}\|} \cdot \mathbf{d_3}, \frac{\pi}{2}\frac{d\rho_\star}{\mu_\star}\|\mathbf{v}_\star - \mathbf{v}\|, \frac{\mu_\star c_{p\star}}{k_\star}\right)(T_\star - T).$$

The (line) heat source $\mathcal{Q}$ acting on a slender body also depends on several material and geometrical properties as well as on the specific inflow situation. The number of dependencies can be reduced to three by help of non-dimensionalizing which yields the dimensionless Nusselt number Nu in dependence of the cosine of the angle of attack, Reynolds and Prandtl numbers. The Reynolds number corresponds to the relative velocity between air flow and glass jet, the typical length is the half jet circumference.

For Nu we use a heuristic model. It originates in the studies of a perpendicular flow around a cylinder [33] and is modified for different inflow directions (angles of attack) with regard to experimental data. A regularization ensures the smooth limit for a transversal incident flow in analogon to the drag model for F

in (3). We apply

$$\mathrm{Nu} : [-1,1] \times \mathbb{R}_0^+ \times \mathbb{R}_0^+ \to \mathbb{R}_0^+ \tag{4}$$

$$\mathrm{Nu}(c,\mathrm{Re},\mathrm{Pr}) = (1 - 0.5\,h^2(c,\mathrm{Re}))\,\left(0.3 + \sqrt{\mathrm{Nu}_{lam}^2(\mathrm{Re},\mathrm{Pr}) + \mathrm{Nu}_{turb}^2(\mathrm{Re},\mathrm{Pr})}\right)$$

$$\mathrm{Nu}_{lam}(\mathrm{Re},\mathrm{Pr}) = 0.664\mathrm{Re}^{1/2}\mathrm{Pr}^{3/2}, \qquad \mathrm{Nu}_{turb}(\mathrm{Re},\mathrm{Pr}) = \frac{0.037\,\mathrm{Re}^{0.9}\mathrm{Pr}}{\mathrm{Re}^{0.1} + 2.443(\mathrm{Pr}^{2/3} - 1)}$$

$$h(c,\mathrm{Re}) = \begin{cases} c\mathrm{Re}/\delta_h & \mathrm{Re} < \delta_h \\ c & \mathrm{Re} \geq \delta_h \end{cases}$$

2.3 Generalization to many rods

In case of k slender bodies in the air flow, we have $\mathbf{\Psi_i}$, $i = 1, ..., k$, representing the quantities of each Cosserat rod, here $k = MN$. Assuming no contact between neighboring fiber jets, every single jet can be described by the stated rod system (1). Their multiple effect on the air flow is reflected in $\mathbf{f}_{jets}$ and q_{jets}. The source terms in the momentum and energy equations of the air flow (2) become

$$\mathbf{f}_{jets}(\mathbf{x},t) = -\sum_{i=1}^{k} \int_{\Gamma_i} \delta(\mathbf{x} - \mathbf{r_i}(s,t))\,\boldsymbol{\mathcal{F}}(\mathbf{\Psi_i}(s,t), \mathbf{\Psi}_\star(\mathbf{x},t))\,\mathrm{d}s$$

$$q_{jets}(\mathbf{x},t) = -\sum_{i=1}^{k} \int_{\Gamma_i} \delta(\mathbf{x} - \mathbf{r_i}(s,t))\,\mathcal{Q}(\mathbf{\Psi_i}(s,t), \mathbf{\Psi}_\star(\mathbf{x},t))\,\mathrm{d}s.$$

3 Models for special set-up of rotational spinning process

In the rotational spinning process under consideration the centrifugal disk is perforated by M rows of N equidistantly placed holes each ($M = 35$, $N = 770$). The spinning conditions (hole size, velocities, temperatures) are thereby identical for each row, see Figure 1. The special set-up allows for the simplification of the general model framework in Section 2. We introduce the rotating outer orthonormal basis $\{\mathbf{a_1}(t), \mathbf{a_2}(t), \mathbf{a_3}(t)\}$ satisfying $\partial_t \mathbf{a_i} = \mathbf{\Omega} \times \mathbf{a_i}$, $i = 1, 2, 3$, where $\mathbf{\Omega}$ is the angular frequency of the centrifugal disk. In particular, $\mathbf{\Omega} = \Omega \mathbf{a_1}$ and $\mathbf{e_g} = -\mathbf{a_1}$ (gravity direction) hold. Then, glass jets and air flow become stationary, presupposing that we consider spun fiber jets of certain length. In particular, we assume the stresses to be vanished at this length. Moreover, the glass jets emerging from the rotating device form dense curtains for every spinning row. As a result of homogenization, we can treat the air flow as rotationally invariant and each curtain can be represented by one jet. This yields an enormous complexity reduction of the problem. The homogenization together with the slender-body theory makes the numerical simulation possible.

3.1 Transition to stationarity

3.1.1 Representative spun jet of certain length

For the viscous Cosserat rods (1), the mass flux is constant in the stationarity, i.e. $uA = Q/\rho = const$. We deal with $\mathbf{\Omega}$-adapted linear and angular velocities, $\mathbf{v}_\Omega = \mathbf{v} - \mathbf{\Omega} \times \mathbf{r}$ and $\boldsymbol{\omega}_\Omega = \boldsymbol{\omega} - \mathbf{\Omega}$, which fulfill the explicit stationarity relations

$$\mathbf{v}_\Omega = u\mathbf{d_3}, \qquad \boldsymbol{\omega}_\Omega = u\boldsymbol{\kappa}$$

resulting from the first two equations of (1). Moreover, fictitious Coriolis and centrifugal forces and associated couples enter the linear and angular momentum equations. Using the material laws we can formulate the stationary rod model in terms of a boundary value problem of first order differential equations. Thereby, we present it in the director basis $\{\mathbf{d_1}, \mathbf{d_2}, \mathbf{d_3}\}$ for convenience (see (5) and compare to [19] except for the

temperature equation). Note that to an arbitrary vector field $\mathbf{z} = \sum_{i=1}^{3} \breve{z}_i \mathbf{a_i} = \sum_{i=1}^{3} z_i \mathbf{d_i} \in \mathbb{E}^3$, we indicate the component tupels corresponding to the rotating outer basis and the director basis by $\breve{\mathsf{z}} = (\breve{z}_1, \breve{z}_2, \breve{z}_3) \in \mathbb{R}^3$ and $\mathsf{z} = (z_1, z_2, z_3) \in \mathbb{R}^3$, respectively. The director basis can be transformed into the rotating outer basis by the tensor-valued rotation $\mathbf{R}$, i.e. $\mathbf{R} = \mathbf{a_i} \otimes \mathbf{d_i} = R_{ij} \mathbf{a_i} \otimes \mathbf{a_j} \in \mathbb{E}^3 \otimes \mathbb{E}^3$ with associated orthogonal matrix $\mathsf{R} = (R_{ij}) = (\mathbf{d_i} \cdot \mathbf{a_j}) \in SO(3)$. Its transpose and inverse matrix is denoted by R^{T}. For the components, $\mathsf{z} = \mathsf{R} \cdot \breve{\mathsf{z}}$ holds. The cross-product $\mathsf{z} \times \mathsf{R}$ is defined as mapping $(\mathsf{z} \times \mathsf{R}) : \mathbb{R}^3 \to \mathbb{R}^3$, $\mathsf{y} \mapsto \mathsf{z} \times (\mathsf{R} \cdot \mathsf{y})$. Moreover, canonical basis vectors in $\mathbb{R}^3$ are denoted by e_i, $i = 1, 2, 3$, e.g. $\mathsf{e}_1 = (1, 0, 0)$. Then, the stationary Cosserat rod model stated in the director basis for a spun glass jet emerging from the centrifugal disk at $s = 0$ with stress-free end at $s = L$ reads

$$
\begin{aligned}
\partial_s \breve{\mathsf{r}} &= \mathsf{R}^{\mathrm{T}} \cdot \mathsf{e}_3 \\
\partial_s \mathsf{R} &= -\kappa \times \mathsf{R} \\
\partial_s \kappa &= -\frac{\rho}{3Q} \frac{\kappa n_3}{\mu} + \frac{4\pi\rho^2}{3Q^2} \frac{u}{\mu} \mathsf{P}_{3/2} \cdot \mathsf{m} \\
\partial_s u &= \frac{\rho}{3Q} \frac{u n_3}{\mu} \\
\partial_s \mathsf{n} &= -\kappa \times \mathsf{n} + Qu\kappa \times \mathsf{e}_3 + \frac{\rho}{3} \frac{u n_3}{\mu} \mathsf{e}_3 + 2Q\Omega (\mathsf{R} \cdot \mathsf{e}_1) \times \mathsf{e}_3 + Q\Omega^2 \frac{1}{u} \mathsf{R} \cdot (\mathsf{e}_1 \times (\mathsf{e}_1 \times \breve{\mathsf{r}})) \\
&\quad + Qg \frac{1}{u} \mathsf{R} \cdot \mathsf{e}_1 - \mathsf{R} \cdot \breve{\mathsf{f}}_{air} \\
\partial_s \mathsf{m} &= -\kappa \times \mathsf{m} + \mathsf{n} \times \mathsf{e}_3 + \frac{\rho}{3} \frac{u}{\mu} \mathsf{P}_3 \cdot \mathsf{m} - \frac{Q}{12\pi} \frac{n_3}{\mu} \mathsf{P}_2 \cdot \kappa - \frac{Q\Omega}{12\pi} \frac{n_3}{\mu u} \mathsf{P}_2 \cdot (\mathsf{R} \cdot \mathsf{e}_1) - \frac{Q^2\Omega}{4\pi\rho} \frac{1}{u} \mathsf{P}_2 \cdot (\kappa \times \mathsf{R} \cdot \mathsf{e}_1) \\
&\quad - \frac{Q^2}{4\pi\rho} \frac{1}{u^2} \mathsf{P}_2 \cdot (u\kappa + \Omega \mathsf{R} \cdot \mathsf{e}_1) \times (u\kappa + \Omega \mathsf{R} \cdot \mathsf{e}_1) \\
\partial_s T &= \frac{1}{c_p Q} (q_{rad} + q_{air})
\end{aligned}
\tag{5}
$$

with $q_{rad} = 2\sqrt{\pi} \varepsilon_R \sigma \sqrt{Q/\rho}\, (T_{ref}^4 - T^4)/\sqrt{u}$ and diagonal matrix $\mathsf{P}_k = \mathrm{diag}(1, 1, k)$, $k \in \mathbb{R}$. It is supplemented with

$$
\breve{\mathsf{r}}(0) = (H, R, 0), \qquad \mathsf{R}(0) = \mathsf{e}_1 \otimes \mathsf{e}_1 - \mathsf{e}_2 \otimes \mathsf{e}_3 + \mathsf{e}_3 \otimes \mathsf{e}_2, \qquad \kappa(0) = \mathsf{0}, \qquad u(0) = U, \qquad T(0) = \theta
$$
$$
\mathsf{n}(L) = \mathsf{0}, \qquad \mathsf{m}(L) = \mathsf{0}
$$

(cf. Table 1). Considering the jet as representative of one spinning row, we choose the nozzle position to be $(H, R, 0)$ with respective height H, R is here the disk radius. The initialization $\mathsf{R}(0)$ prescribes the jet direction at the nozzle as $(\mathbf{d_1}, \mathbf{d_2}, \mathbf{d_3})(0) = (\mathbf{a_1}, -\mathbf{a_3}, \mathbf{a_2})$.

Remark 1. *The rotations $\mathsf{R} \in SO(3)$ can be parameterized, e.g. in Euler angles or unit quaternions [39]. The last variant offers a very elegant way of rewriting the second equation of* (5)*. Define*

$$
\mathsf{R}(\mathsf{q}) = \begin{pmatrix} q_1^2 - q_2^2 - q_3^2 + q_0^2 & 2(q_1 q_2 - q_0 q_3) & 2(q_1 q_3 + q_0 q_2) \\ 2(q_1 q_2 + q_0 q_3) & -q_1^2 + q_2^2 - q_3^2 + q_0^2 & 2(q_2 q_3 - q_0 q_1) \\ 2(q_1 q_3 - q_0 q_2) & 2(q_2 q_3 + q_0 q_1) & -q_1^2 - q_2^2 + q_3^2 + q_0^2 \end{pmatrix}, \ \mathsf{q} = (q_0, q_1, q_2, q_3),
$$

with $\|\mathsf{q}\| = 1$, then we have $\partial_s \mathsf{q} = \mathcal{A}(\kappa) \cdot \mathsf{q}$ with skew-symmetric matrix

$$
\mathcal{A}(\mathsf{z}) = \frac{1}{2} \begin{pmatrix} 0 & z_1 & z_2 & z_3 \\ -z_1 & 0 & z_3 & -z_2 \\ -z_2 & -z_3 & 0 & z_1 \\ -z_3 & z_2 & -z_1 & 0 \end{pmatrix}.
$$

3.1.2 Rotationally invariant air flow

Due to the spinning set-up the jets emerging from the rotating device form row-wise dense curtains. As a consequence of a row-wise homogenization, the air flow (2) can be treated as stationary not only in the rotating outer basis $\{\mathbf{a_1}(t), \mathbf{a_2}(t), \mathbf{a_3}(t)\}$, but also in a fixed outer one. Because of the symmetry with respect to the rotation axis, it is convenient to introduce cylindrical coordinates $(x, r, \phi) \in \mathbb{R} \times \mathbb{R}^+ \times [0, 2\pi)$ for the space and to attach a cylindrical basis $\{\mathbf{e_x}, \mathbf{e_r}, \mathbf{e_\phi}\}$ with $\mathbf{e_x} = \mathbf{a_1}$ to each space point. The components to an arbitrary vector field $\mathbf{z} \in \mathbb{E}^3$ are indicated by $\hat{\mathbf{z}} = (z_x, z_r, z_\phi) \in \mathbb{R}^3$. Then, taking advantage of the rotational invariance, the stationary Navier-Stokes equations in (x, r) simplify to

$$
\begin{aligned}
&\partial_x(\rho_\star v_{x\star}) + \frac{1}{r}\partial_r(r\rho_\star v_{r\star}) = 0 \qquad (6)\\
&\partial_x(\rho_\star v_{x\star}^2) + \frac{1}{r}\partial_r(r\rho_\star v_{r\star} v_{x\star})\\
&\quad = -\partial_x p_\star + \partial_x(2\mu_\star \partial_x v_{x\star} + \lambda_\star \nabla\cdot\hat{\mathbf{v}}_\star) + \frac{1}{r}\partial_r(r\mu_\star(\partial_x v_{r\star} + \partial_r v_{x\star})) - \rho_\star g + (f_x)_{jets}\\
&\partial_x(\rho_\star v_{x\star} v_{r\star}) + \frac{1}{r}\partial_r(r\rho_\star v_{r\star}^2) - \frac{1}{r}\rho_\star v_{\phi\star}^2\\
&\quad = -\partial_r p_\star + \partial_x(\mu_\star(\partial_x v_{r\star} + \partial_r v_{x\star})) + \frac{2}{r}\partial_r(r\mu_\star \partial_r v_{r\star}) + \partial_r(\lambda_\star \nabla\cdot\hat{\mathbf{v}}_\star) - \frac{2}{r^2}\mu_\star v_{r\star} + (f_r)_{jets}\\
&\partial_x(\rho_\star v_{x\star} v_{\phi\star}) + \frac{1}{r}\partial_r(r\rho_\star v_{r\star} v_{\phi\star}) + \frac{1}{r}\rho_\star v_{r\star} v_{\phi\star} = \partial_x(\mu_\star \partial_x v_{\phi\star}) + \frac{1}{r^2}\partial_r(r^3\mu_\star \partial_r(\frac{1}{r}v_{\phi\star})) + (f_\phi)_{jets}\\
&\partial_x(\rho_\star e_\star v_{x\star}) + \frac{1}{r}\partial_r(r\rho_\star e_\star v_{r\star})\\
&\quad = -p_\star \nabla\cdot\hat{\mathbf{v}}_\star + \mu_\star(2(\partial_x v_{x\star})^2 + 2(\partial_r v_{r\star})^2 + (\partial_x v_{r\star} + \partial_r v_{x\star})^2 + (\partial_x v_{\phi\star})^2 + (r\partial_r(\frac{1}{r}v_{r\star}))^2 + \frac{2}{r^2}v_{r\star}^2)\\
&\qquad + \lambda_\star(\nabla\cdot\hat{\mathbf{v}}_\star)^2 + \partial_x(k_\star \partial_x T_\star) + \frac{1}{r}\partial_r(r k_\star \partial_r T_\star) + q_{jets}
\end{aligned}
$$

with $\nabla\cdot\hat{\mathbf{v}}_\star = \partial_x v_{x\star} + (\partial_r(r v_{r\star}))/r$ and equipped with appropriate inflow, outflow and wall boundary conditions, cf. Figure 1.

3.2 Exchange functions

To perform the coupling between (5) and (6), we have to compute the exchange functions in the appropriate coordinates. These calculations are simplified by the rotational invariance of the problem. As introduced, we use the subscripts $\breve{}$ and $\hat{}$ to indicate the component tupels corresponding to the rotating outer basis $\{\mathbf{a_1}(t), \mathbf{a_2}(t), \mathbf{a_3}(t)\}$ and the cylindrical basis $\{\mathbf{e_x}, \mathbf{e_r}, \mathbf{e}_\phi\}$, respectively. Essentially for the coupling are the jet tangent and the relative velocity between air flow and glass jet, they are

$$
\breve{\tau} = \mathsf{R}^{\mathrm{T}} \cdot \mathsf{e}_3, \qquad \hat{\tau} = \left(\breve{\tau}_1, \frac{\breve{r}_2\breve{\tau}_2 + \breve{r}_3\breve{\tau}_3}{\sqrt{\breve{r}_2^2 + \breve{r}_3^2}}, \frac{\breve{r}_2\breve{\tau}_3 - \breve{r}_3\breve{\tau}_2}{\sqrt{\breve{r}_2^2 + \breve{r}_3^2}}\right),
$$

$$
\breve{\mathbf{v}}_{rel} = \left(v_{x\star}, \frac{\breve{r}_2 v_{r\star} - \breve{r}_3(v_{\phi\star} - \Omega r)}{\sqrt{\breve{r}_2^2 + \breve{r}_3^2}}, \frac{\breve{r}_3 v_{r\star} + \breve{r}_2(v_{\phi\star} - \Omega r)}{\sqrt{\breve{r}_2^2 + \breve{r}_3^2}}\right) - u\breve{\tau}, \qquad \hat{\mathbf{v}}_{rel} = (v_{x\star}, v_{r\star}, v_{\phi\star} - \Omega r) - u\hat{\tau}.
$$

Then, the drag forces are

$$\breve{\mathsf{f}}_{air}(s) = \breve{\mathcal{F}}(\Psi(s), \Psi_\star(\breve{r}_1(s), \sqrt{\breve{r}_2^2(s) + \breve{r}_3^2(s)}))$$

$$\hat{\mathsf{f}}_{jets}(x,r) = -\frac{N}{2\pi}\int_I \frac{1}{r}\,\delta(x-\breve{r}_1(s))\,\delta(r-\sqrt{\breve{r}_2^2(s)+\breve{r}_3^2(s)})\;\hat{\mathcal{F}}(\Psi(s),\Psi_\star(x,r))\,\mathrm{d}s$$

$$\breve{\mathcal{F}}(\Psi,\Psi_\star) = 2\sqrt{\frac{Q}{\pi\rho}}\frac{\mu_\star^2}{\rho_\star}\frac{1}{\sqrt{u}}\,\mathrm{F}\left(\breve{\tau}, 2\sqrt{\frac{Q}{\pi\rho}}\frac{\rho_\star}{\mu_\star}\frac{1}{\sqrt{u}}\breve{\mathfrak{v}}_{rel}\right), \quad \hat{\mathcal{F}}(\Psi,\Psi_\star) = 2\sqrt{\frac{Q}{\pi\rho}}\frac{\mu_\star^2}{\rho_\star}\frac{1}{\sqrt{u}}\,\mathrm{F}\left(\hat{\tau}, 2\sqrt{\frac{Q}{\pi\rho}}\frac{\rho_\star}{\mu_\star}\frac{1}{\sqrt{u}}\hat{\mathfrak{v}}_{rel}\right)$$

and the heat sources

$$q_{air}(s) = \mathcal{Q}(\Psi(s), \Psi_\star(\breve{r}_1(s), \sqrt{\breve{r}_2^2(s) + \breve{r}_3^2(s)}))$$

$$q_{jets}(x,r) = -\frac{N}{2\pi}\int_I \frac{1}{r}\,\delta(x-\breve{r}_1(s))\,\delta(r-\sqrt{\breve{r}_2^2(s)+\breve{r}_3^2(s)})\;\mathcal{Q}(\Psi(s),\Psi_\star(x,r))\,\mathrm{d}s$$

$$\mathcal{Q}(\Psi,\Psi_\star) = 2k_\star\,\mathrm{Nu}\left(\frac{\breve{\mathfrak{v}}_{rel}}{\|\breve{\mathfrak{v}}_{rel}\|}\cdot\breve{\tau}, \sqrt{\frac{\pi Q}{\rho}}\frac{\rho_\star}{\mu_\star}\frac{1}{\sqrt{u}}\|\breve{\mathfrak{v}}_{rel}\|, \frac{\mu_\star c_{p\star}}{k_\star}\right)(T_\star - T).$$

Here, $\hat{\mathsf{f}}_{jets}$ and q_{jets} represent the homogenized effect of the N glass jets emerging from the equidistantly placed holes in an arbitrary spinning row. Correspondingly, system (5) with $\breve{\mathsf{f}}_{air}$ and q_{air} describes one representative glass jet for this row. To simulate the full problem with all MN glass jets in the air, jet representatives Ψ_i, $i = 1, ..., M$ for all M spinning rows with the respective boundary and air flow conditions have to be determined. Their common effect on the air flow is (cf. Section 2.3)

$$\hat{\mathsf{f}}_{jets}(x,r) = -\frac{N}{2\pi}\sum_{i=1}^{M}\int_{I_i} \frac{1}{r}\,\delta(x-\breve{r}_{1,i}(s))\,\delta(r-\sqrt{\breve{r}_{2,i}^2(s)+\breve{r}_{3,i}^2(s)})\;\hat{\mathcal{F}}(\Psi_i(s),\Psi_\star(x,r))\,\mathrm{d}s$$

$$q_{jets}(x,r) = -\frac{N}{2\pi}\sum_{i=1}^{M}\int_{I_i} \frac{1}{r}\,\delta(x-\breve{r}_{1,i}(s))\,\delta(r-\sqrt{\breve{r}_{2,i}^2(s)+\breve{r}_{3,i}^2(s)})\;\mathcal{Q}(\Psi_i(s),\Psi_\star(x,r))\,\mathrm{d}s.$$

4 Numerical treatment

The numerical simulation of the glass jets dynamic in the air flow is performed by an algorithm that weakly couples glass jet calculation and air flow computation via iterations. This procedure is adequate for the problem and has the advantage that we can combine commercial software and self-implemented code. We use FLUENT, a commercial finite volume-based software by ANSYS, that contains the broad physical modeling capabilities needed to describe air flow, turbulence and heat transfer for the industrial glass wool manufacturing process. In particular, a pressure-based solver is applied in the computation of (6). To restrict the computational effort in grid refinement needed for the resolution of the turbulent air streams we consider alternatively a stochastic k-ω turbulence model.[2] Note that this modification of the model equations has no effect on our coupling framework, where the exchange functions are incorporated by UDFs (user defined functions). For the boundary value problem of the stationary Cosserat rod (5), systems of nonlinear equations are set up via a Runge-Kutta collocation method and solved by a Newton method in MATLAB 7.4. The convergence of the Newton method depends thereby crucially on the initial guess. To improve the computational performance we adapt the initial guess iteratively by solving a sequence of boundary value problems with slightly changed parameters. The developed continuation method is presented in Section 4.1. Moreover, to get a balanced numerics we use the dimensionless rod system that is scaled with the respective conditions at the nozzle. The M glass jet representative are computed in parallel. The exchange of flow and fiber data between the solvers is based on interpolation and averaging, as we explain in the weak iterative coupling algorithm in Section 4.2.

[2]For details on the commercial software FLUENT, its models and solvers we refer to `http://www.fluent.com`.

4.1 Collocation-continuation method for dimensionless rod boundary value problem

The computing of the glass jets is based on a dimensionless rod system. For this purpose, we scale the dimensional equations (5) with the spinning conditions of the respective row. Apart from the air flow data, (5) contains thirteen physical parameters, i.e. jet density ρ, heat capacity c_p, emissivity ε_R, typical length L, velocity U and temperature θ at the spinning hole as well as hole diameter D and height H, centrifugal disk radius R, rotational frequency Ω, reference temperature for radiation T_{ref} and gravitational acceleration g. The typical jet viscosity is chosen to be $\mu_0 = \mu(\theta)$. These induce various dimensionless numbers characterizing the fiber spinning, i.e. Reynolds number Re as ratio between inertia and viscosity, Rossby number Rb as ratio between inertia and rotation, Froude number Fr as ratio between inertia and gravity and Ra as ratio between radiation and heat advection as well as ℓ, h and ϵ as length ratios between jet length, hole height, diameter and disk radius, respectively

$$\mathrm{Re} = \frac{\rho U R}{\mu_0}, \qquad \mathrm{Rb} = \frac{U}{\Omega R}, \qquad \mathrm{Fr} = \frac{U}{\sqrt{gR}}, \qquad \mathrm{Ra} = \frac{4\varepsilon_R \sigma \theta^3 R}{\rho c_p U D}, \qquad \ell = \frac{L}{R}, \qquad h = \frac{H}{R}, \qquad \epsilon = \frac{D}{R}.$$

In addition, we introduce dimensionless quantities that also depend on local air flow data, similarly to the Nusselt number in (4)

$$\mathrm{A}_1 = \frac{4\mu_\star^2 R}{\pi \rho_\star \rho U^2 D^3}, \quad \mathrm{A}_2 = \frac{\rho_\star U D}{\mu_\star} \quad \mathrm{A}_3 = \frac{8 k_\star R}{\pi \rho c_p \theta D^2}, \quad \mathrm{A}_4 = \frac{\mu_\star c_{p\star}}{k_\star}.$$

Here, A_4 is the Prandtl number of the air flow. To make (5) dimensionless we use the following reference values:

$$\begin{aligned} &s_0 = L, \qquad r_0 = R, \qquad \kappa_0 = R^{-1}, \qquad u_0 = U, \qquad T_0 = \theta \\ &\mu_0 = \mu(T_0), \qquad n_0 = \pi \mu_0 U D^2/(4R), \qquad m_0 = \pi \mu_0 U D^4/(16R^2). \end{aligned}$$

We choose the disk radius R as macroscopic length scale in the scalings, since it is well known by the set-up. As for L, we consider jet lengths where the stresses are supposed to be vanished. In general, R and L are of same order such that the parameter ϵ can be identified with the slenderness ratio δ of the jets, cf. Section 1. The last two scalings for n_0 and m_0 are motivated by the material laws and the fact that the mass flux is $Q = \pi \rho U D^2/4$. Then, the dimensionless system for the stationary viscous rod has the form

$$\begin{aligned}
&\frac{1}{\ell}\partial_s \breve{\mathsf{r}} = \mathsf{R}^{\mathrm{T}} \cdot \mathsf{e}_3 = \breve{\tau} \\
&\frac{1}{\ell}\partial_s \mathsf{R} = -\kappa \times \mathsf{R} \\
&\frac{1}{\ell}\partial_s \kappa = -\frac{1}{3\mu}\kappa n_3 + \frac{4}{3\mu} u \mathsf{P}_{3/2} \cdot \mathsf{m} \\
&\frac{1}{\ell}\partial_s u = \frac{1}{3\mu} u n_3 \\
&\frac{1}{\ell}\partial_s \mathsf{n} = -\kappa \times \mathsf{n} + \mathrm{Re}\, u \left(\kappa \times \mathsf{e}_3 + \frac{1}{3\mu} n_3 \mathsf{e}_3 \right) + \frac{2\mathrm{Re}}{\mathrm{Rb}} (\mathsf{R} \cdot \mathsf{e}_1) \times \mathsf{e}_3 + \frac{\mathrm{Re}}{\mathrm{Rb}^2} \frac{1}{u} \mathsf{R} \cdot (\mathsf{e}_1 \times (\mathsf{e}_1 \times \breve{\mathsf{r}})) \\
&\qquad + \frac{\mathrm{Re}}{\mathrm{Fr}^2} \frac{1}{u} \mathsf{R} \cdot \mathsf{e}_1 - \mathrm{Re}\, \mathrm{A}_1 \sqrt{u} \mathsf{R} \cdot \mathrm{F}\left(\breve{\tau}, \mathrm{A}_2 \frac{1}{\sqrt{u}} \breve{\mathsf{v}}_{rel} \right) \\
&\frac{1}{\ell}\partial_s \mathsf{m} = -\kappa \times \mathsf{m} + \frac{4}{\epsilon^2} \mathsf{n} \times \mathsf{e}_3 + \frac{\mathrm{Re}}{3\mu} \left(u \mathsf{P}_3 \cdot \mathsf{m} - \frac{1}{4} n_3 \mathsf{P}_2 \cdot \kappa \right) - \frac{\mathrm{Re}}{4\mathrm{Rb}} \frac{1}{u} \mathsf{P}_2 \cdot \left(\frac{1}{3\mu} \mathsf{R} \cdot \mathsf{e}_1 n_3 + \kappa \times \mathsf{R} \cdot \mathsf{e}_1 \right) \\
&\qquad - \frac{\mathrm{Re}}{4} \left(\frac{1}{u^2} \mathsf{P}_2 \cdot (u\kappa + \frac{1}{\mathrm{Rb}} \mathsf{R} \cdot \mathsf{e}_1) \right) \times \left(u\kappa + \frac{1}{\mathrm{Rb}} \mathsf{R} \cdot \mathsf{e}_1 \right) \\
&\frac{1}{\ell}\partial_s T = \mathrm{Ra} \frac{1}{\sqrt{u}} (T_{ref}^4 - T^4) + \mathrm{A}_3\, \mathrm{Nu} \left(\frac{\breve{\mathsf{v}}_{rel}}{\|\breve{\mathsf{v}}_{rel}\|} \cdot \breve{\tau}, \frac{\pi}{2} \mathrm{A}_2 \frac{1}{\sqrt{u}} \|\breve{\mathsf{v}}_{rel}\|, \mathrm{A}_4 \right) (T_\star - T),
\end{aligned} \tag{7}$$

with

$$\check{\mathsf{r}}(0) = (h, 1, 0), \qquad \mathsf{R}(0) = \mathsf{e}_1 \otimes \mathsf{e}_1 - \mathsf{e}_2 \otimes \mathsf{e}_3 + \mathsf{e}_3 \otimes \mathsf{e}_2, \qquad \kappa(0) = 0, \qquad u(0) = 1, \qquad T(0) = 1$$
$$\mathsf{n}(1) = 0, \qquad \mathsf{m}(1) = 0.$$

Here, T_{ref} and the air flow associated $T_\star$ and $\check{\mathsf{v}}_{rel}$ are scaled with θ and U, respectively. System (7) contains the slenderness parameter ϵ ($\epsilon \ll 1$) explicity in the equation for the couple m and is hence no asymptotic model of zeroth order. In the slenderness limit $\epsilon \to 0$, the rod model reduces to a string system and their solutions for $(\check{\mathsf{r}}, \check{\tau}, u, N = n_3, T)$ coincide. Only these jet quantities are relevant for the two-way coupling, as they enter in the exchange functions. However, the simpler string system is not well-posed for all parameter ranges, [15, 16]. Thus, it makes sense to consider (7) as ϵ-regularized string system, [19]. We treat ϵ as moderate fixed regularization parameter in the following to stabilize the numerics, in particular we set $\epsilon = 0.1$.

For the numerical treatment of (7), systems of non-linear equations are set up via a Runge-Kutta collocation method and solved by a Newton method. The Runge-Kutta collocation method is an integration scheme of fourth order for boundary value problems, i.e. $\partial_s \mathsf{z} = \mathsf{f}(s, \mathsf{z})$, $\mathsf{f} : [a, b] \times \mathbb{R}^n \to \mathbb{R}^n$ with $\mathsf{g}(\mathsf{z}(a), \mathsf{z}(b)) = 0$. It is a standard routine in MATLAB 7.4 with adaptive grid refinement (solver `bvp4c.m`). Let $a = s_0 < s_1 < ... < s_N = b$ be the collocation points in $[a, b]$ with $h_i = s_i - s_{i-1}$ and denote $\mathsf{z}_\mathsf{i} = \mathsf{z}(s_i)$. Then, the nonlinear system of $(N + 1)$ equations, $\mathsf{S}(\mathsf{z}^h) = 0$, for the discrete solution $\mathsf{z}^h = (\mathsf{z}_\mathsf{i})_{i=0,...,N}$ is set up via

$$\mathsf{S}_0(\mathsf{z}^h) = \mathsf{g}(\mathsf{z}_0, \mathsf{z}_\mathsf{N}) = 0$$
$$\mathsf{S}_{\mathsf{i}+1}(\mathsf{z}^h) = \mathsf{z}_{\mathsf{i}+1} - \mathsf{z}_\mathsf{i} - \frac{h_{i+1}}{6}\left(\mathsf{f}(s_i, \mathsf{z}_\mathsf{i}) + 4\mathsf{f}(s_{i+1/2}, \mathsf{z}_{\mathsf{i}+1/2}) + \mathsf{f}(s_{i+1}, \mathsf{z}_{\mathsf{i}+1})\right) = 0,$$
$$\mathsf{z}_{\mathsf{i}+1/2} = \frac{1}{2}\left(\mathsf{z}_{\mathsf{i}+1} + \mathsf{z}_\mathsf{i}\right) - \frac{h_{i+1}}{8}\left(\mathsf{f}(s_{i+1}, \mathsf{z}_{\mathsf{i}+1}) - \mathsf{f}(s_i, \mathsf{z}_\mathsf{i})\right)$$

for $i = 0, ..., N - 1$. The convergence and hence the computational performance of the Newton method depends crucially on the initial guess. Thus, we adapt the initial guess iteratively by help of a continuation strategy. We scale the drag function F with the factor $\mathrm{C_F^{-2}}$ and the right-hand side of the temperature equation with C_T and treat Re, Rb, Fr, ℓ, $\mathrm{C_F}$ and C_T as continuation parameters. We start from the solution for $(\mathrm{Re}, \mathrm{Rb}, \mathrm{Fr}, \ell, \mathrm{C_F}, \mathrm{C}_T) = (1, 1, 1, 0.15, \infty, 0)$ which corresponds to an isothermal rod without aerodynamic forces that has been intensively numerically investigated in [19]. Its determination is straight forward using the related string model as initial guess. Note that we choose ℓ so small to ensure that the glass jet lies in the air flow domain. The actual continuation is then divided into three parts. First, $(\mathrm{Re}, \mathrm{Rb}, \mathrm{Fr}, \mathrm{C_F})$ are adjusted, then C_T and finally ℓ. In the continuation we use an adaptive step size control. Thereby, we always compute the interim solutions by help of one step and two half steps and decide with regard to certain quality criteria whether the step size should be increased or decreased.

4.2 Weak iterative coupling algorithm

The numerical difficulty of the coupling of glass jet and air flow computations, $\mathcal{S}_{jets}$ and $\mathcal{S}_{air}$, results from the different underlying discretizations. Let I_h denote the rod grid used in the continuation method and I_Δ be an equidistant grid of step size Δs with respective jet data Ψ_Δ for data exchange. Moreover, let Ω_h denote the finite volume mesh with the flow data $\Psi_{\star,V}$ for the cell V. For the air associated exchange functions, the flow data is linearly interpolated on I_h. Precisely, the linear interpolation $\mathbb{L}$ with respect to $\check{\mathsf{r}}(s_j)$, $s_j \in I_h$ is performed over all $V \in \mathcal{N}(s_j)$, where $\mathcal{N}(s_j)$ is the set of the cell containing $\check{\mathsf{r}}(s_j)$ and its direct neighbor cells,

$$\check{\mathsf{f}}_{air}(s_j) \approx \check{\mathcal{F}}(\Psi(s_j), \mathbb{L}_{\mathcal{N}(s_j)}[\Psi_{\star,V}]), \qquad q_{air}(s_j) \approx \mathcal{Q}(\Psi(s_j), \mathbb{L}_{\mathcal{N}(s_j)}[\Psi_{\star,V}]).$$

For the jet associated exchange functions entering the finite volume scheme, we need the averaged jet information for every cell $V \in \Omega_h$. We introduce $I_{\Delta,V} = \{s_j \in I_\Delta | \check{\mathsf{r}}(s_j) \in V\}$ and $|I_V| = \Delta s |I_{\Delta,V}|$, then the

averaging $\mathbb{E}$ with respect to V is performed over the $I_{\Delta,V}$-associated data,

$$\frac{2\pi}{|V|}\int_V r\,\hat{\mathsf{f}}_{jets}(x,r)\,\mathrm{d}x\,\mathrm{d}r \approx -\frac{N|I_V|}{|V|}\,\hat{\mathcal{F}}(\mathbb{E}_V[\Psi_\Delta],\Psi_{\star,V}),$$
$$\frac{2\pi}{|V|}\int_V r\,q_{jets}(x,r)\,\mathrm{d}x\,\mathrm{d}r \approx -\frac{N|I_V|}{|V|}\,\mathcal{Q}(\mathbb{E}_V[\Psi_\Delta],\Psi_{\star,V}).$$

The ratio $|I_V|/|V|$ can be considered as the jet length density for the cell V. In case of M jet representatives, we deal with $I_{\Delta,V,i}$ and $|I_{V,i}|$ for $i = 1,...,M$. Consequently, we have $I_{\Delta,V} = \cup_{i=1}^M I_{\Delta,V,i}$ and $|I_V| = \sum_{i=1}^M |I_{V,i}|$. Note, that the interpolation and averaging approximation strategies have the disadvantage that they are qualitatively different. Thus, momentum and energy conservation are only ensured for very fine resolutions.

Summing up, the algorithm that we use to couple glass jet $\mathcal{S}_{jets}$ and air flow $\mathcal{S}_{air}$ computations has the form:

Algorithm 1.
Generate flow mesh Ω_h
Perform flow simulation $\mathcal{S}_{air}$ *without jets to obtain* $\Psi_\star^{(0)}$
Initialize $k = 0$
Do
- *Compute:* $\Psi_i^{(k)} = \mathcal{S}_{jets}(\Psi_\star^{(k)})$ *for* $i = 1,...,M$
  where flow data is linearly interpolated on I_h
- *Interpolate jet data on equidistant grid* I_Δ
- *Find for every cell* V *in* Ω_h *the relevant rod points* $I_{\Delta,V}$ *and average the respective data*
- *Compute:* $\Psi_\star^{(k+1)} = \mathcal{S}_{air}(\Psi^{(k)})$
- *Update:* $k = k + 1$

while $\|\Psi^{(k)} - \Psi^{(k-1)}\| > tol$

Remark 2. *From the technical point of view, the efficient management of the simulation and coupling routines is quite demanding. In a preprocessing step we generate the finite volume mesh* Ω_h *via the software Gambit and save it in a file that is available for FLUENT and MATLAB. The program of Algorithm 1 is then realized with FLUENT as master tool. After the air flow simulation FLUENT starts MATLAB. MATLAB governs the parallelization of the jets computation via MATLAB executables. Collecting the jets information, it provides the averaged jets data on* Ω_h *in a file. FLUENT reads in this data and performs a new air flow simulation with immersed jets.*

5 Results

In this section we illustrate the applicability of our asymptotic coupling framework to the given rotational spinning process. We show the convergence of the weak iterative coupling algorithm and discuss the effects of the fluid-fiber-interactions.

For all air flow simulations we use the same finite volume mesh Ω_h whose refinement levels are initially chosen according to the unperturbed flow structure, independently of the glass jets. This implies a very fine resolution at the injector of the turbulent cross flow which is coarsen towards the centrifugal disk. For mesh details see Figure 2 (left). The turbulent intensity is visualized in Figure 2 (right). As expected it is high at the injector and moderate in the remaining flow domain. In particular, it is less than 2% in the region near the centrifugal disk where the glass jets will be presumably located. Thus, we neglect turbulence effects on the jets dynamics in the following. However, note that such effects can be easily incorporated by help of stochastic drag models [24, 37, 40] that are based on RANS turbulence descriptions (e.g. k-ϵ model or k-ω model). For the jet computations the grid I_h is automatically generated and adapted by the continuation method in every iteration. To ensure that sufficient jet points lie in each flow cell and a proper data exchange

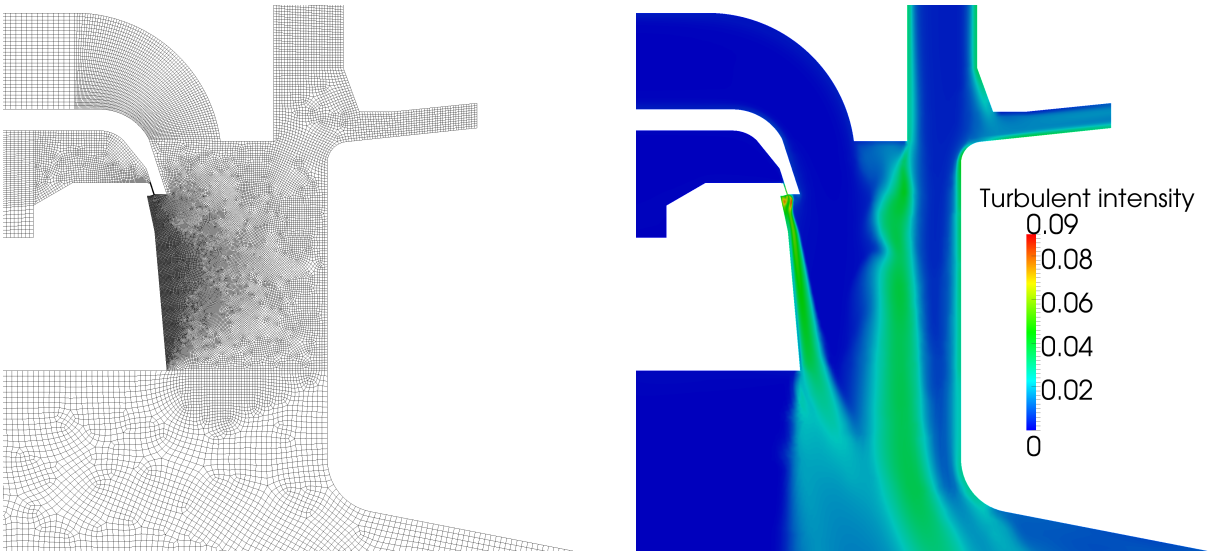

Figure 2: *Left:* finite volume mesh Ω_h for air flow computations (mesh detail). *Right:* turbulent intensity of the air flow.

is given we use an equidistant grid I_Δ with appropriate step size Δs, (at minimum 2 jet points per interacting flow cell).

The weak iterative coupling algorithm is fully automated. Each iteration starts with the same initialization. There is no parameter adjustment. The algorithm turns out to be very robust and reliable in spite of coarse flow meshs. For our set-up an air flow simulation takes around 30 minutes CPU-time, and the computation of a single jet takes approximatively just as long. The algorithm converges within 12-14 iterations. Figure 3 shows the relative $\mathcal{L}^2$-error of all jet curve components over the number of iterations k, i.e.

$$\sum_{i=1}^{M} \frac{\|\breve{r}_{j,i}^{(k)} - \breve{r}_{j,i}^{f}\|_{\mathcal{L}^2(I_i)}}{\|\breve{r}_{j,i}^{f}\|_{\mathcal{L}^2(I_i)}}, \quad \text{with } \breve{r}_{j,i}^{f} \text{ final solution}, \qquad j = 1, 2, 3.$$

The effects of the fluid-fiber interactions and the necessity of the two-way coupling procedure for the rotational spinning process can be concluded from the following results. Figure 4 shows the swirl velocity of the air flow and the location of the immersed glass jets over the iterations. In the unperturbed flow without the glass jets there is no swirl velocity. In fact, the presence of the jets cause the swirl velocity, since the jets pull the flow with them. Moreover, the jets deflect the downwards directed burner flow, as seen in Figure 5. The jets behavior looks very reasonable. Trajectories and positions are as expected. Furthermore, their properties, i.e. velocity u and temperature T, correspond to the axial flow velocity and flow temperature, which implies a proper momentum and heat exchange. For jet details we refer to Figure 6. It shows the influence of the spinning rows. The jet representative of the highest spinning row is warmer than the one of the lowest row which implies better stretching capabilities. It is also faster and hence thinner ($A = u^{-1}$). This certainly comes from the fact that the highest jet is longer affected by the fast hot burner flow. However, in view of quality assessment, slenderness and homogeneity of the spun fiber jets play an important role. This requires the optimal design of the spinning conditions, e.g. different nozzle diameters or various distances between spinning rows. But for this purpose, also the melting regime has to be taken into account in modeling and simulation which is left to future research.

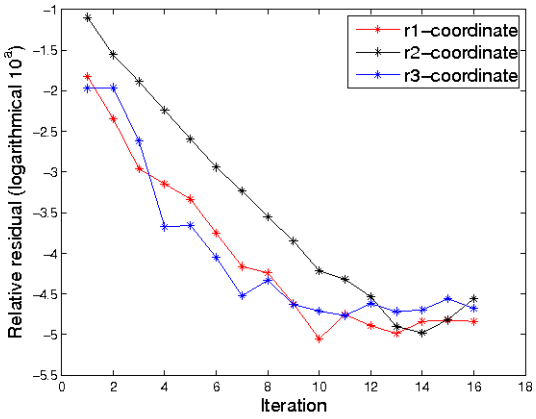

Figure 3: Convergence of the weak iterative coupling algorithm. Relative error of all M curve coordinates in $\mathcal{L}^2(I)$-norm over number of iterations, plotted in logarithmic scale.

6 Conclusion

The optimal design of rotational spinning processes for glass wool manufacturing involves the simulation of ten thousands of slender viscous thermal glass jets in fast air streams. This is a computational challenge where direct numerical methods fail. In this paper we have established an asymptotic modeling concept for the fluid-fiber interactions. Based on slender-body theory and homogenization it reduces the complexity of the problem enormously and makes numerical simulations possible. Adequate to problem and model we have proposed an algorithm that weakly couples air flow and glass jets computations via iterations. It turns out to be very robust and converges to reasonable results within few iterations. Moreover, the possibility of combining commercial software and self-implemented code yields satisfying efficiency off-the-shelf. The performance might certainly be improved even more by help of future studies. Summing up, our developed asymptotic coupling framework provides a very promising basis for future optimization strategies.

In view of the design of the whole production process the melting regime must be taken into account in modeling and simulation. Melting and spinning regimes influence each other. On one hand the conditions at the spinning rows are crucially affected by the melt distribution in the centrifugal disk and the burner air flow, regarding e.g. cooling by mixing inside, aerodynamic heating outside. On the other hand the burner flow and the arising heat distortion of the disk are affected by the spun jet curtains. This obviously demands a further coupling procedure.

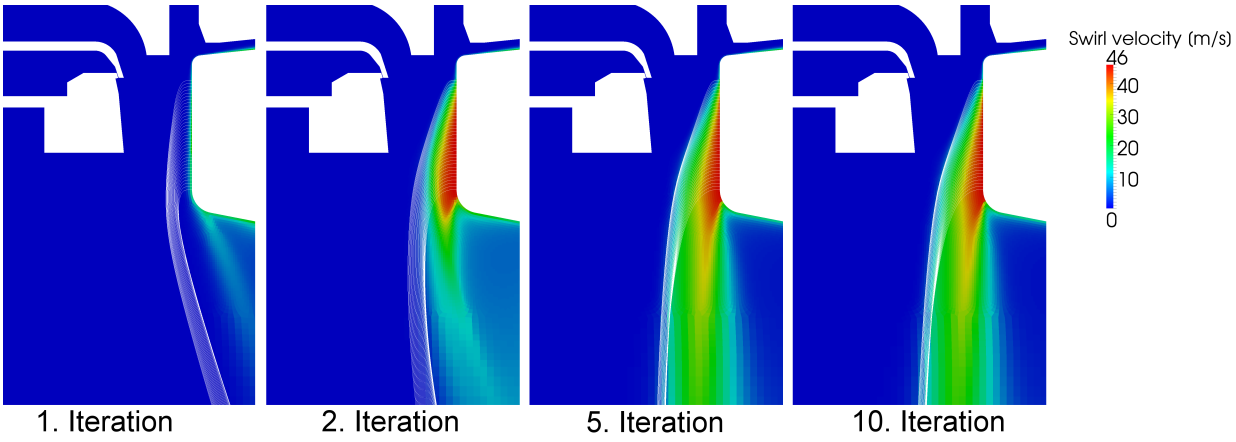

Figure 4: Illustration of iterative coupling procedure. Iteration results for air swirl velocity and immersed glass jets (plotted as white curves).

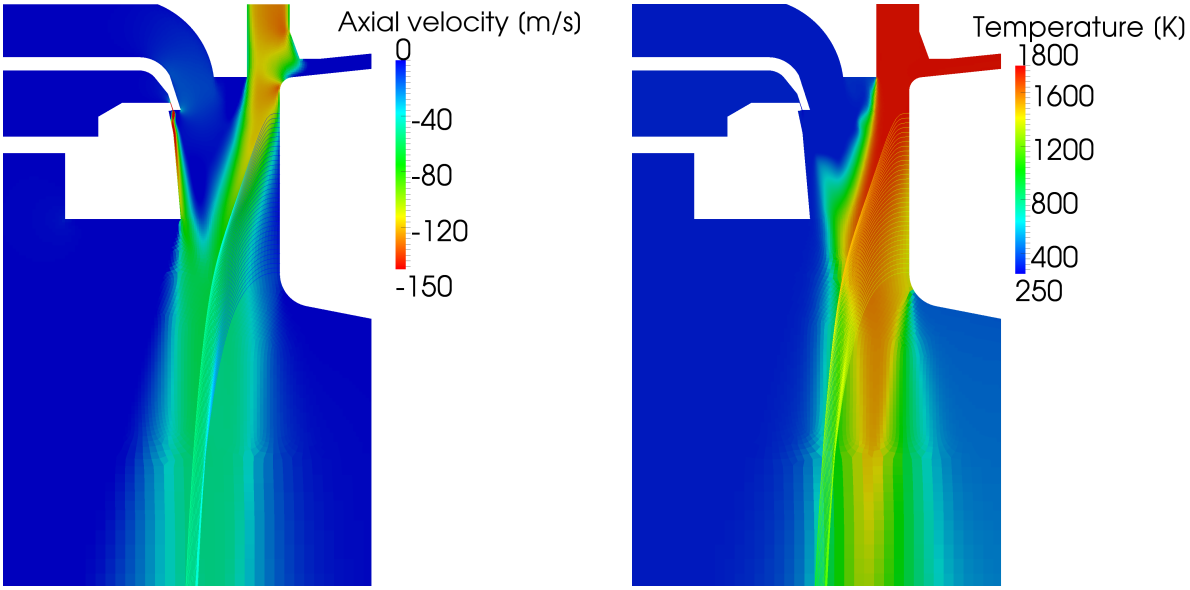

Figure 5: Final simulation result. Glass jets and air flow in given rotational spinning process. The color maps visualize axial velocity and temperature of the air flow, respectively. In addition, the immersed $M = 35$ glass jet representatives are colored with respect to their corresponding quantities, i.e. u and T. The dynamics and properties of the highest and lowest jets are shown in detail in Figure 6.

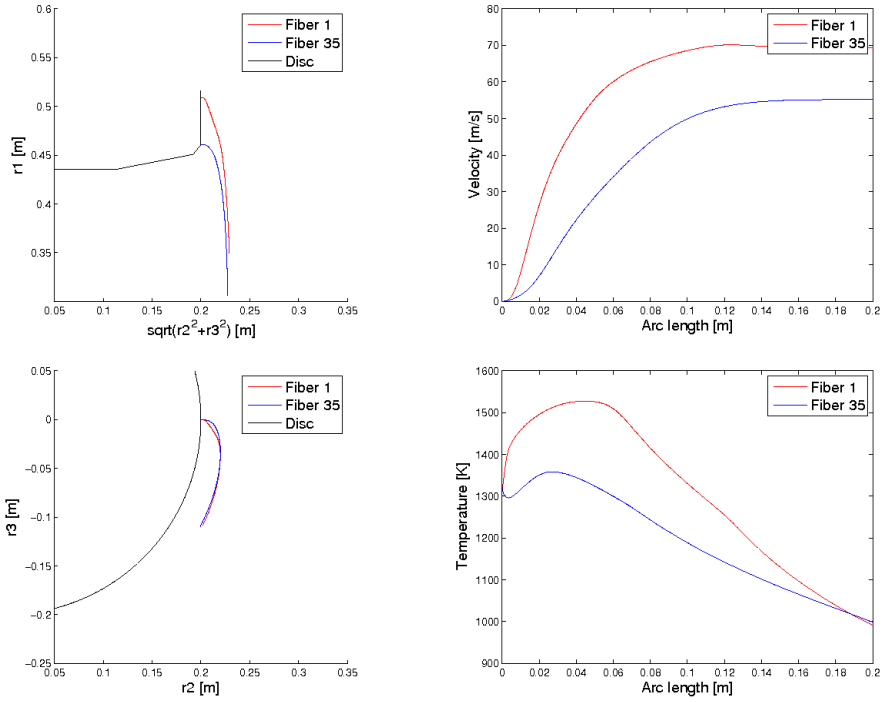

Figure 6: Dynamics of the jets emerging from the highest and lowest spinning rows of the centrifugal disk. Left: side and top view of the plant. Right: jets velocity $u(s)$ and temperature $T(s)$, $s \in [0, L]$.

Acknowledgments

We would like to acknowledge our industrial partner, the company Woltz GmbH in Wertheim, for the interesting and challenging problem. This work has been supported by German Bundesministerium für Bildung und Forschung, Schwerpunkt "Mathematik für Innovationen in Industrie und Dienstleistungen", Projekt 03MS606 and by German Bundesministerium für Wirtschaft und Technologie, Förderprogramm ZIM, Projekt AUROFA 114626.

References

1. Klar A, Marheinke N, Wegener R: **Hierarchy of mathematical models for production processes of technical textiles**. *ZAMM - J. Appl. Math. Mech.* 2009, **89**:941–961.
2. Pearson JRA: *Mechanics of Polymer Processing*. Elsevier 1985.
3. Decent SP, King AC, Simmons MJH, Parau EI, Wallwork IM, Gurney CJ, Uddin J: **The trajectory and stability of a spiralling liquid jet: Viscous theory**. *Appl. Math. Mod.* 2009, **33**(12):4283–4302.
4. Parau EI, Decent SP, King AC, Simmons MJH, Wong D: **Nonlinear viscous liquid jets from a rotating orifice**. *J. Eng. Math.* 2006, **57**:159–179.
5. Marheineke N, Wegener R: **Asymptotic model for the dynamics of curved viscous fibers with surface tension**. *J. Fluid. Mech.* 2009, **622**:345–369.
6. Antman SS: *Nonlinear Problems of Elasticity*. New York: Springer 2006.
7. Entov VM, Yarin AL: **The dynamics of thin liquid jets in air**. *J. Fluid. Mech.* 1984, **140**:91–111.
8. Yarin AL: *Free Liquid Jets and Films: Hydrodynamics and Rheology*. New York: Longman 1993.

9. Cummings LJ, Howell PD: **On the evolution of non-axissymetric viscous fibres with surface tension inertia and gravity**. *J. Fluid. Mech.* 1999, **389**:361–389.
10. Dewynne JN, Howell PD, Wilmott P: **Slender viscous fibers with inertia and gravity**. *Quart. J. Mech. Appl. Math.* 1994, **47**:541–555.
11. Dewynne JN, Ockendon JR, Wilmott P: **A systematic derivation of the leading-order equations for extensional flows in slender geometries**. *J. Fluid. Mech.* 1992, **244**:323–338.
12. Decent SP, King AC, Wallwork IM: **Free jets spun from a prilling tower**. *J. Eng. Math.* 2002, **42**:265–282.
13. Panda S, Marheineke N, Wegener R: **Systematic derivation of an asymptotic model for the dynamics of curved viscous fibers**. *Math. Meth. Appl. Sci.* 2008, **31**:1153–1173.
14. Wallwork IM, Decent SP, King AC, Schulkes RMSM: **The trajectory and stability of a spiralling liquid jet. Part 1. Inviscid theory**. *J. Fluid. Mech.* 2002, **459**:43–65.
15. Götz T, Klar A, Unterreiter A, Wegener R: **Numerical evidence for the non-existence of solutions to the equations describing rotational fiber spinning**. *Math. Mod. Meth. Appl. Sci.* 2008, **18**(10):1829–1844.
16. Arne W, Marheineke N, Meister A, Wegener R: **Numerical analysis of Cosserat rod and string models for viscous jets in rotational spinning processes**. *Math. Mod. Meth. Appl. Sci.* 2010, **20**(10):1941–1965.
17. Hlod A, Aarts ACT, van de Ven AAF, Peletier MA: **Mathematical model of falling of a viscous jet onto a moving surface18**:659–677.
18. Hlod A, Aarts ACT, van de Ven AAF, Peletier MA: **Three flow regimes of viscous jet falling onto a moving surface**. *arxiv:0811.2574* 2008.
19. Arne W, Marheineke N, Wegener R: **Asymptotic transition of Cosserat rod to string models for curved viscous inertial jets**. *Berichte des Fraunhofer ITWM* 2010, **192**.
20. Ribe NM: **Coiling of viscous jets**. *Proc. Roy. Soc. London A* 2004, **2051**:3223–3239.
21. Ribe NM, Habibi M, Bonn D: **Stability of liquid rope coiling**. *Phys. Fluids* 2006, **18**:084102.
22. Chiu-Webster S, Lister JR: **The fall of a viscous thread onto a moving surface: A 'fluid-mechanical sewing machine'**. *J. Fluid. Mech.* 2006, **569**:89–111.
23. Ribe NM, Lister JR, Chiu-Webster S: **Stability of a dragged viscous thread: Onset of 'stitching' in a fluid-mechanical 'sewing machine'**. *Phys. Fluids* 2006, **18**:124105.
24. Marheineke N, Wegener R: **Modeling and application of a stochastic drag for fiber dynamics in turbulent flows**. *Int. J. Multiphase Flow* 2010, **doi**:10.1016/j.ijmultiphaseflow.2010.10.001.
25. Tomotika S, Aoi T, Yosinobu H: **On the forces acting on a circular cylinder set obliquely in a uniform stream at low values of Reynolds number**. *Proc. Roy. Soc. London A* 1953, **219**(1137):233–244.
26. Batchelor GK: **Slender-body theory for particles of arbitrary cross-section in Stokes flow**. *J. Fluid. Mech.* 1970, **44**(3):419–440.
27. Cox RG: **The motion of long slender bodies in a viscous fluid. Part 1. General theory**. *J. Fluid. Mech.* 1970, **44**(4):791–810.
28. Taylor GI: **Analysis of the swimming of long and narrow animals**. *Proc. Roy. Soc. London A* 1952, **214**:158–183.
29. Sumer BM, Fredsoe J: *Hydrodynamics around Cylindrical Structures*. World Scientific Publishing 2006.
30. Schlichting H: *Grenzschicht-Theorie*. Karlsruhe: Verlag G. Braun 1982.
31. Schewe G: **On the force fluctuations acting on a circular cylinder in cross-flow from subcritical up to transcritical Reynolds numbers**. *J. Fluid. Mech.* 1983, **133**:265–285.
32. Tritton DJ: **Experiments on the flow past circular cylinder at low Reynolds number**. *J. Fluid. Mech.* 1959, **6**:547–567.
33. VDI-Gesellschaft: *VDI-Wärmeatlas*. Springer, 10 edition 2006.
34. Ribe NM, Huppert HE, Hallworth MA, Habibi M, Bonn D: **Multiple coexisting states of liquid rope coiling**. *J. Fluid. Mech.* 2006, **555**:275–297.
35. Ferziger JH, Perić M: *Computational Methods for Fluid Dynamics*. Berlin: Springer, 3 edition 2002.

36. Zdravkovich MM: *Flow around Circular Cylinders, Vol 1: Fundamentals*. New York: Oxford University Press 1997.

37. Marheineke N, Wegener R: **Fiber dynamics in turbulent flows: General modeling framework**. *SIAM J. Appl. Math.* 2006, **66**(5):1703–1726.

38. Hoerner SF: **Fluid-dynamic drag. Practical information on aerodynamic drag and hydrodynamic resistance**. *Published by the author. Obtainable from ISVA*. 1965.

39. Mahadevan L, Keller JB: **Coiling of flexible ropes**. *Proc. Roy. Soc. London A* 1996, **452**:1679–1694.

40. Marheineke N, Wegener R: **Fiber dynamics in turbulent flows: Specific Taylor drag**. *SIAM J. Appl. Math.* 2007, **68**:1–23.

Published reports of the Fraunhofer ITWM

The PDF-files of the following reports are available under:
www.itwm.fraunhofer.de/de/zentral__berichte/berichte

1. D. Hietel, K. Steiner, J. Struckmeier
A Finite - Volume Particle Method for Compressible Flows
(19 pages, 1998)

2. M. Feldmann, S. Seibold
Damage Diagnosis of Rotors: Application of Hilbert Transform and Multi-Hypothesis Testing
Keywords: Hilbert transform, damage diagnosis, Kalman filtering, non-linear dynamics
(23 pages, 1998)

3. Y. Ben-Haim, S. Seibold
Robust Reliability of Diagnostic Multi-Hypothesis Algorithms: Application to Rotating Machinery
Keywords: Robust reliability, convex models, Kalman filtering, multi-hypothesis diagnosis, rotating machinery, crack diagnosis
(24 pages, 1998)

4. F.-Th. Lentes, N. Siedow
Three-dimensional Radiative Heat Transfer in Glass Cooling Processes
(23 pages, 1998)

5. A. Klar, R. Wegener
A hierarchy of models for multilane vehicular traffic
Part I: Modeling
(23 pages, 1998)

Part II: Numerical and stochastic investigations
(17 pages, 1998)

6. A. Klar, N. Siedow
Boundary Layers and Domain Decomposition for Radiative Heat Transfer and Diffusion Equations: Applications to Glass Manufacturing Processes
(24 pages, 1998)

7. I. Choquet
Heterogeneous catalysis modelling and numerical simulation in rarified gas flows Part I: Coverage locally at equilibrium
(24 pages, 1998)

8. J. Ohser, B. Steinbach, C. Lang
Efficient Texture Analysis of Binary Images
(17 pages, 1998)

9. J. Orlik
Homogenization for viscoelasticity of the integral type with aging and shrinkage
(20 pages, 1998)

10. J. Mohring
Helmholtz Resonators with Large Aperture
(21 pages, 1998)

11. H. W. Hamacher, A. Schöbel
On Center Cycles in Grid Graphs
(15 pages, 1998)

12. H. W. Hamacher, K.-H. Küfer
Inverse radiation therapy planning - a multiple objective optimisation approach
(14 pages, 1999)

13. C. Lang, J. Ohser, R. Hilfer
On the Analysis of Spatial Binary Images
(20 pages, 1999)

14. M. Junk
On the Construction of Discrete Equilibrium Distributions for Kinetic Schemes
(24 pages, 1999)

15. M. Junk, S. V. Raghurame Rao
A new discrete velocity method for Navier-Stokes equations
(20 pages, 1999)

16. H. Neunzert
Mathematics as a Key to Key Technologies
(39 pages, 1999)

17. J. Ohser, K. Sandau
Considerations about the Estimation of the Size Distribution in Wicksell's Corpuscle Problem
(18 pages, 1999)

18. E. Carrizosa, H. W. Hamacher, R. Klein, S. Nickel
Solving nonconvex planar location problems by finite dominating sets
Keywords: Continuous Location, Polyhedral Gauges, Finite Dominating Sets, Approximation, Sandwich Algorithm, Greedy Algorithm
(19 pages, 2000)

19. A. Becker
A Review on Image Distortion Measures
Keywords: Distortion measure, human visual system
(26 pages, 2000)

20. H. W. Hamacher, M. Labbé, S. Nickel, T. Sonneborn
Polyhedral Properties of the Uncapacitated Multiple Allocation Hub Location Problem
Keywords: integer programming, hub location, facility location, valid inequalities, facets, branch and cut
(21 pages, 2000)

21. H. W. Hamacher, A. Schöbel
Design of Zone Tariff Systems in Public Transportation
(30 pages, 2001)

22. D. Hietel, M. Junk, R. Keck, D. Teleaga
The Finite-Volume-Particle Method for Conservation Laws
(16 pages, 2001)

23. T. Bender, H. Hennes, J. Kalcsics, M. T. Melo, S. Nickel
Location Software and Interface with GIS and Supply Chain Management
Keywords: facility location, software development, geographical information systems, supply chain management
(48 pages, 2001)

24. H. W. Hamacher, S. A. Tjandra
Mathematical Modelling of Evacuation Problems: A State of Art
(44 pages, 2001)

25. J. Kuhnert, S. Tiwari
Grid free method for solving the Poisson equation
Keywords: Poisson equation, Least squares method, Grid free method
(19 pages, 2001)

26. T. Götz, H. Rave, D. Reinel-Bitzer, K. Steiner, H. Tiemeier
Simulation of the fiber spinning process
Keywords: Melt spinning, fiber model, Lattice Boltzmann, CFD
(19 pages, 2001)

27. A. Zemitis
On interaction of a liquid film with an obstacle
Keywords: impinging jets, liquid film, models, numerical solution, shape
(22 pages, 2001)

28. I. Ginzburg, K. Steiner
Free surface lattice-Boltzmann method to model the filling of expanding cavities by Bingham Fluids
Keywords: Generalized LBE, free-surface phenomena, interface boundary conditions, filling processes, Bingham viscoplastic model, regularized models
(22 pages, 2001)

29. H. Neunzert
»Denn nichts ist für den Menschen als Menschen etwas wert, was er nicht mit Leidenschaft tun kann«
Vortrag anlässlich der Verleihung des Akademiepreises des Landes Rheinland-Pfalz am 21.11.2001
Keywords: Lehre, Forschung, angewandte Mathematik, Mehrskalenanalyse, Strömungsmechanik
(18 pages, 2001)

30. J. Kuhnert, S. Tiwari
Finite pointset method based on the projection method for simulations of the incompressible Navier-Stokes equations
Keywords: Incompressible Navier-Stokes equations, Meshfree method, Projection method, Particle scheme, Least squares approximation
AMS subject classification: 76D05, 76M28
(25 pages, 2001)

31. R. Korn, M. Krekel
Optimal Portfolios with Fixed Consumption or Income Streams
Keywords: Portfolio optimisation, stochastic control, HJB equation, discretisation of control problems
(23 pages, 2002)

32. M. Krekel
Optimal portfolios with a loan dependent credit spread
Keywords: Portfolio optimisation, stochastic control, HJB equation, credit spread, log utility, power utility, non-linear wealth dynamics
(25 pages, 2002)

33. J. Ohser, W. Nagel, K. Schladitz
The Euler number of discretized sets – on the choice of adjacency in homogeneous lattices
Keywords: image analysis, Euler number, neighborhod relationships, cuboidal lattice
(32 pages, 2002)

34. I. Ginzburg, K. Steiner
Lattice Boltzmann Model for Free-Surface flow and Its Application to Filling Process in Casting
Keywords: Lattice Boltzmann models; free-surface phenomena; interface boundary conditions; filling processes; injection molding; volume of fluid method; interface boundary conditions; advection-schemes; upwind-schemes
(54 pages, 2002)

35. M. Günther, A. Klar, T. Materne, R. Wegener
Multivalued fundamental diagrams and stop and go waves for continuum traffic equations
Keywords: traffic flow, macroscopic equations, kinetic derivation, multivalued fundamental diagram, stop and go waves, phase transitions
(25 pages, 2002)

36. S. Feldmann, P. Lang, D. Prätzel-Wolters
Parameter influence on the zeros of network determinants
Keywords: Networks, Equicofactor matrix polynomials, Realization theory, Matrix perturbation theory
(30 pages, 2002)

37. K. Koch, J. Ohser, K. Schladitz
Spectral theory for random closed sets and estimating the covariance via frequency space
Keywords: Random set, Bartlett spectrum, fast Fourier transform, power spectrum
(28 pages, 2002)

38. D. d'Humières, I. Ginzburg
Multi-reflection boundary conditions for lattice Boltzmann models
Keywords: lattice Boltzmann equation, boudary condistions, bounce-back rule, Navier-Stokes equation
(72 pages, 2002)

39. R. Korn
Elementare Finanzmathematik
Keywords: Finanzmathematik, Aktien, Optionen, Portfolio-Optimierung, Börse, Lehrerweiterbildung, Mathematikunterricht
(98 pages, 2002)

40. J. Kallrath, M. C. Müller, S. Nickel
Batch Presorting Problems: Models and Complexity Results
Keywords: Complexity theory, Integer programming, Assigment, Logistics
(19 pages, 2002)

41. J. Linn
On the frame-invariant description of the phase space of the Folgar-Tucker equation
Key words: fiber orientation, Folgar-Tucker equation, injection molding
(5 pages, 2003)

42. T. Hanne, S. Nickel
A Multi-Objective Evolutionary Algorithm for Scheduling and Inspection Planning in Software Development Projects
Key words: multiple objective programming, project management and scheduling, software development, evolutionary algorithms, efficient set
(29 pages, 2003)

43. T. Bortfeld , K.-H. Küfer, M. Monz, A. Scherrer, C. Thieke, H. Trinkaus
Intensity-Modulated Radiotherapy - A Large Scale Multi-Criteria Programming Problem
Keywords: multiple criteria optimization, representative systems of Pareto solutions, adaptive triangulation, clustering and disaggregation techniques, visualization of Pareto solutions, medical physics, external beam radiotherapy planning, intensity modulated radiotherapy
(31 pages, 2003)

44. T. Halfmann, T. Wichmann
Overview of Symbolic Methods in Industrial Analog Circuit Design
Keywords: CAD, automated analog circuit design, symbolic analysis, computer algebra, behavioral modeling, system simulation, circuit sizing, macro modeling, differential-algebraic equations, index
(17 pages, 2003)

45. S. E. Mikhailov, J. Orlik
Asymptotic Homogenisation in Strength and Fatigue Durability Analysis of Composites
Keywords: multiscale structures, asymptotic homogenization, strength, fatigue, singularity, non-local conditions
(14 pages, 2003)

46. P. Domínguez-Marín, P. Hansen, N. Mladenovic , S. Nickel
Heuristic Procedures for Solving the Discrete Ordered Median Problem
Keywords: genetic algorithms, variable neighborhood search, discrete facility location
(31 pages, 2003)

47. N. Boland, P. Domínguez-Marín, S. Nickel, J. Puerto
Exact Procedures for Solving the Discrete Ordered Median Problem
Keywords: discrete location, Integer programming
(41 pages, 2003)

48. S. Feldmann, P. Lang
Padé-like reduction of stable discrete linear systems preserving their stability
Keywords: Discrete linear systems, model reduction, stability, Hankel matrix, Stein equation
(16 pages, 2003)

49. J. Kallrath, S. Nickel
A Polynomial Case of the Batch Presorting Problem
Keywords: batch presorting problem, online optimization, competetive analysis, polynomial algorithms, logistics
(17 pages, 2003)

50. T. Hanne, H. L. Trinkaus
knowCube for MCDM – Visual and Interactive Support for Multicriteria Decision Making
Key words: Multicriteria decision making, knowledge management, decision support systems, visual interfaces, interactive navigation, real-life applications.
(26 pages, 2003)

51. O. Iliev, V. Laptev
On Numerical Simulation of Flow Through Oil Filters
Keywords: oil filters, coupled flow in plain and porous media, Navier-Stokes, Brinkman, numerical simulation
(8 pages, 2003)

52. W. Dörfler, O. Iliev, D. Stoyanov, D. Vassileva
On a Multigrid Adaptive Refinement Solver for Saturated Non-Newtonian Flow in Porous Media
Keywords: Nonlinear multigrid, adaptive refinement, non-Newtonian flow in porous media
(17 pages, 2003)

53. S. Kruse
On the Pricing of Forward Starting Options under Stochastic Volatility
Keywords: Option pricing, forward starting options, Heston model, stochastic volatility, cliquet options
(11 pages, 2003)

54. O. Iliev, D. Stoyanov
Multigrid – adaptive local refinement solver for incompressible flows
Keywords: Navier-Stokes equations, incompressible flow, projection-type splitting, SIMPLE, multigrid methods, adaptive local refinement, lid-driven flow in a cavity
(37 pages, 2003)

55. V. Starikovicius
The multiphase flow and heat transfer in porous media
Keywords: Two-phase flow in porous media, various formulations, global pressure, multiphase mixture model, numerical simulation
(30 pages, 2003)

56. P. Lang, A. Sarishvili, A. Wirsen
Blocked neural networks for knowledge extraction in the software development process
Keywords: Blocked Neural Networks, Nonlinear Regression, Knowledge Extraction, Code Inspection
(21 pages, 2003)

57. H. Knaf, P. Lang, S. Zeiser
Diagnosis aiding in Regulation Thermography using Fuzzy Logic
Keywords: fuzzy logic,knowledge representation, expert system
(22 pages, 2003)

58. M. T. Melo, S. Nickel, F. Saldanha da Gama
Largescale models for dynamic multicommodity capacitated facility location
Keywords: supply chain management, strategic planning, dynamic location, modeling
(40 pages, 2003)

59. J. Orlik
Homogenization for contact problems with periodically rough surfaces
Keywords: asymptotic homogenization, contact problems
(28 pages, 2004)

60. A. Scherrer, K.-H. Küfer, M. Monz, F. Alonso, T. Bortfeld
IMRT planning on adaptive volume structures – a significant advance of computational complexity
Keywords: Intensity-modulated radiation therapy (IMRT), inverse treatment planning, adaptive volume structures, hierarchical clustering, local refinement, adaptive clustering, convex programming, mesh generation, multi-grid methods
(24 pages, 2004)

61. D. Kehrwald
Parallel lattice Boltzmann simulation of complex flows
Keywords: Lattice Boltzmann methods, parallel computing, microstructure simulation, virtual material design, pseudo-plastic fluids, liquid composite moulding
(12 pages, 2004)

62. O. Iliev, J. Linn, M. Moog, D. Niedziela, V. Starikovicius
On the Performance of Certain Iterative Solvers for Coupled Systems Arising in Discretization of Non-Newtonian Flow Equations

Keywords: Performance of iterative solvers, Preconditioners, Non-Newtonian flow
(17 pages, 2004)

63. R. Ciegis, O. Iliev, S. Rief, K. Steiner
On Modelling and Simulation of Different Regimes for Liquid Polymer Moulding
Keywords: Liquid Polymer Moulding, Modelling, Simulation, Infiltration, Front Propagation, non-Newtonian flow in porous media
(43 pages, 2004)

64. T. Hanne, H. Neu
Simulating Human Resources in Software Development Processes
Keywords: Human resource modeling, software process, productivity, human factors, learning curve
(14 pages, 2004)

65. O. Iliev, A. Mikelic, P. Popov
Fluid structure interaction problems in deformable porous media: Toward permeability of deformable porous media
Keywords: fluid-structure interaction, deformable porous media, upscaling, linear elasticity, stokes, finite elements
(28 pages, 2004)

66. F. Gaspar, O. Iliev, F. Lisbona, A. Naumovich, P. Vabishchevich
On numerical solution of 1-D poroelasticity equations in a multilayered domain
Keywords: poroelasticity, multilayered material, finite volume discretization, MAC type grid
(41 pages, 2004)

67. J. Ohser, K. Schladitz, K. Koch, M. Nöthe
Diffraction by image processing and its application in materials science
Keywords: porous microstructure, image analysis, random set, fast Fourier transform, power spectrum, Bartlett spectrum
(13 pages, 2004)

68. H. Neunzert
Mathematics as a Technology: Challenges for the next 10 Years
Keywords: applied mathematics, technology, modelling, simulation, visualization, optimization, glass processing, spinning processes, fiber-fluid interaction, trubulence effects, topological optimization, multicriteria optimization, Uncertainty and Risk, financial mathematics, Malliavin calculus, Monte-Carlo methods, virtual material design, filtration, bio-informatics, system biology
(29 pages, 2004)

69. R. Ewing, O. Iliev, R. Lazarov, A. Naumovich
On convergence of certain finite difference discretizations for 1D poroelasticity interface problems
Keywords: poroelasticity, multilayered material, finite volume discretizations, MAC type grid, error estimates
(26 pages,2004)

70. W. Dörfler, O. Iliev, D. Stoyanov, D. Vassileva
On Efficient Simulation of Non-Newtonian Flow in Saturated Porous Media with a Multigrid Adaptive Refinement Solver
Keywords: Nonlinear multigrid, adaptive renement, non-Newtonian in porous media
(25 pages, 2004)

71. J. Kalcsics, S. Nickel, M. Schröder
Towards a Unified Territory Design Approach – Applications, Algorithms and GIS Integration
Keywords: territory desgin, political districting, sales territory alignment, optimization algorithms, Geographical Information Systems
(40 pages, 2005)

72. K. Schladitz, S. Peters, D. Reinel-Bitzer, A. Wiegmann, J. Ohser
Design of acoustic trim based on geometric modeling and flow simulation for non-woven
Keywords: random system of fibers, Poisson line process, flow resistivity, acoustic absorption, Lattice-Boltzmann method, non-woven
(21 pages, 2005)

73. V. Rutka, A. Wiegmann
Explicit Jump Immersed Interface Method for virtual material design of the effective elastic moduli of composite materials
Keywords: virtual material design, explicit jump immersed interface method, effective elastic moduli, composite materials
(22 pages, 2005)

74. T. Hanne
Eine Übersicht zum Scheduling von Baustellen
Keywords: Projektplanung, Scheduling, Bauplanung, Bauindustrie
(32 pages, 2005)

75. J. Linn
The Folgar-Tucker Model as a Differetial Algebraic System for Fiber Orientation Calculation
Keywords: fiber orientation, Folgar–Tucker model, invariants, algebraic constraints, phase space, trace stability
(15 pages, 2005)

76. M. Speckert, K. Dreßler, H. Mauch, A. Lion, G. J. Wierda
Simulation eines neuartigen Prüfsystems für Achserprobungen durch MKS-Modellierung einschließlich Regelung
Keywords: virtual test rig, suspension testing, multibody simulation, modeling hexapod test rig, optimization of test rig configuration
(20 pages, 2005)

77. K.-H. Küfer, M. Monz, A. Scherrer, P. Süss, F. Alonso, A. S. A. Sultan, Th. Bortfeld, D. Craft, Chr. Thieke
Multicriteria optimization in intensity modulated radiotherapy planning
Keywords: multicriteria optimization, extreme solutions, real-time decision making, adaptive approximation schemes, clustering methods, IMRT planning, reverse engineering
(51 pages, 2005)

78. S. Amstutz, H. Andrä
A new algorithm for topology optimization using a level-set method
Keywords: shape optimization, topology optimization, topological sensitivity, level-set
(22 pages, 2005)

79. N. Ettrich
Generation of surface elevation models for urban drainage simulation
Keywords: Flooding, simulation, urban elevation models, laser scanning
(22 pages, 2005)

80. H. Andrä, J. Linn, I. Matei, I. Shklyar, K. Steiner, E. Teichmann
OPTCAST – Entwicklung adäquater Strukturoptimierungsverfahren für Gießereien Technischer Bericht (KURZFASSUNG)
Keywords: Topologieoptimierung, Level-Set-Methode, Gießprozesssimulation, Gießtechnische Restriktionen, CAE-Kette zur Strukturoptimierung
(77 pages, 2005)

81. N. Marheineke, R. Wegener
Fiber Dynamics in Turbulent Flows Part I: General Modeling Framework
Keywords: fiber-fluid interaction; Cosserat rod; turbulence modeling; Kolmogorov's energy spectrum; double-velocity correlations; differentiable Gaussian fields
(20 pages, 2005)

Part II: Specific Taylor Drag
Keywords: flexible fibers; k-ε turbulence model; fiber-turbulence interaction scales; air drag; random Gaussian aerodynamic force; white noise; stochastic differential equations; ARMA process
(18 pages, 2005)

82. C. H. Lampert, O. Wirjadi
An Optimal Non-Orthogonal Separation of the Anisotropic Gaussian Convolution Filter
Keywords: Anisotropic Gaussian filter, linear filtering, orientation space, nD image processing, separable filters
(25 pages, 2005)

83. H. Andrä, D. Stoyanov
Error indicators in the parallel finite element solver for linear elasticity DDFEM
Keywords: linear elasticity, finite element method, hierarchical shape functions, domain decom-position, parallel implementation, a posteriori error estimates
(21 pages, 2006)

84. M. Schröder, I. Solchenbach
Optimization of Transfer Quality in Regional Public Transit
Keywords: public transit, transfer quality, quadratic assignment problem
(16 pages, 2006)

85. A. Naumovich, F. J. Gaspar
On a multigrid solver for the three-dimensional Biot poroelasticity system in multilayered domains
Keywords: poroelasticity, interface problem, multigrid, operator-dependent prolongation
(11 pages, 2006)

86. S. Panda, R. Wegener, N. Marheineke
Slender Body Theory for the Dynamics of Curved Viscous Fibers
Keywords: curved viscous fibers; fluid dynamics; Navier-Stokes equations; free boundary value problem; asymptotic expansions; slender body theory
(14 pages, 2006)

87. E. Ivanov, H. Andrä, A. Kudryavtsev
Domain Decomposition Approach for Automatic Parallel Generation of Tetrahedral Grids
Key words: Grid Generation, Unstructured Grid, Delaunay Triangulation, Parallel Programming, Domain Decomposition, Load Balancing
(18 pages, 2006)

88. S. Tiwari, S. Antonov, D. Hietel, J. Kuhnert, R. Wegener
A Meshfree Method for Simulations of Interactions between Fluids and Flexible Structures
Key words: Meshfree Method, FPM, Fluid Structure Interaction, Sheet of Paper, Dynamical Coupling
(16 pages, 2006)

89. R. Ciegis , O. Iliev, V. Starikovicius, K. Steiner
Numerical Algorithms for Solving Problems of Multiphase Flows in Porous Media
Keywords: nonlinear algorithms, finite-volume method, software tools, porous media, flows
(16 pages, 2006)

90. D. Niedziela, O. Iliev, A. Latz
On 3D Numerical Simulations of Viscoelastic Fluids
Keywords: non-Newtonian fluids, anisotropic viscosity, integral constitutive equation
(18 pages, 2006)

91. A. Winterfeld
Application of general semi-infinite Programming to Lapidary Cutting Problems
Keywords: large scale optimization, nonlinear programming, general semi-infinite optimization, design centering, clustering
(26 pages, 2006)

92. J. Orlik, A. Ostrovska
Space-Time Finite Element Approximation and Numerical Solution of Hereditary Linear Viscoelasticity Problems
Keywords: hereditary viscoelasticity; kern approximation by interpolation; space-time finite element approximation, stability and a priori estimate
(24 pages, 2006)

93. V. Rutka, A. Wiegmann, H. Andrä
EJIIM for Calculation of effective Elastic Moduli in 3D Linear Elasticity
Keywords: Elliptic PDE, linear elasticity, irregular domain, finite differences, fast solvers, effective elastic moduli
(24 pages, 2006)

94. A. Wiegmann, A. Zemitis
EJ-HEAT: A Fast Explicit Jump Harmonic Averaging Solver for the Effective Heat Conductivity of Composite Materials
Keywords: Stationary heat equation, effective thermal conductivity, explicit jump, discontinuous coefficients, virtual material design, microstructure simulation, EJ-HEAT
(21 pages, 2006)

95. A. Naumovich
On a finite volume discretization of the three-dimensional Biot poroelasticity system in multilayered domains
Keywords: Biot poroelasticity system, interface problems, finite volume discretization, finite difference method
(21 pages, 2006)

96. M. Krekel, J. Wenzel
A unified approach to Credit Default Swaption and Constant Maturity Credit Default Swap valuation
Keywords: LIBOR market model, credit risk, Credit Default Swaption, Constant Maturity Credit Default Swap-method
(43 pages, 2006)

97. A. Dreyer
Interval Methods for Analog Circiuts
Keywords: interval arithmetic, analog circuits, tolerance analysis, parametric linear systems, frequency response, symbolic analysis, CAD, computer algebra
(36 pages, 2006)

98. N. Weigel, S. Weihe, G. Bitsch, K. Dreßler
Usage of Simulation for Design and Optimization of Testing
Keywords: Vehicle test rigs, MBS, control, hydraulics, testing philosophy
(14 pages, 2006)

99. H. Lang, G. Bitsch, K. Dreßler, M. Speckert
Comparison of the solutions of the elastic and elastoplastic boundary value problems
Keywords: Elastic BVP, elastoplastic BVP, variational inequalities, rate-independency, hysteresis, linear kinematic hardening, stop- and play-operator
(21 pages, 2006)

100. M. Speckert, K. Dreßler, H. Mauch
MBS Simulation of a hexapod based suspension test rig
Keywords: Test rig, MBS simulation, suspension, hydraulics, controlling, design optimization
(12 pages, 2006)

101. S. Azizi Sultan, K.-H. Küfer
A dynamic algorithm for beam orientations in multicriteria IMRT planning
Keywords: radiotherapy planning, beam orientation optimization, dynamic approach, evolutionary algorithm, global optimization
(14 pages, 2006)

102. T. Götz, A. Klar, N. Marheineke, R. Wegener
A Stochastic Model for the Fiber Lay-down Process in the Nonwoven Production
Keywords: fiber dynamics, stochastic Hamiltonian system, stochastic averaging
(17 pages, 2006)

103. Ph. Süss, K.-H. Küfer
Balancing control and simplicity: a variable aggregation method in intensity modulated radiation therapy planning
Keywords: IMRT planning, variable aggregation, clustering methods
(22 pages, 2006)

104. A. Beaudry, G. Laporte, T. Melo, S. Nickel
Dynamic transportation of patients in hospitals
Keywords: in-house hospital transportation, dial-a-ride, dynamic mode, tabu search
(37 pages, 2006)

105. Th. Hanne
Applying multiobjective evolutionary algorithms in industrial projects
Keywords: multiobjective evolutionary algorithms, discrete optimization, continuous optimization, electronic circuit design, semi-infinite programming, scheduling
(18 pages, 2006)

106. J. Franke, S. Halim
Wild bootstrap tests for comparing signals and images
Keywords: wild bootstrap test, texture classification, textile quality control, defect detection, kernel estimate, nonparametric regression
(13 pages, 2007)

107. Z. Drezner, S. Nickel
Solving the ordered one-median problem in the plane
Keywords: planar location, global optimization, ordered median, big triangle small triangle method, bounds, numerical experiments
(21 pages, 2007)

108. Th. Götz, A. Klar, A. Unterreiter, R. Wegener
Numerical evidance for the non-existing of solutions of the equations desribing rotational fiber spinning
Keywords: rotational fiber spinning, viscous fibers, boundary value problem, existence of solutions
(11 pages, 2007)

109. Ph. Süss, K.-H. Küfer
Smooth intensity maps and the Bortfeld-Boyer sequencer
Keywords: probabilistic analysis, intensity modulated radiotherapy treatment (IMRT), IMRT plan application, step-and-shoot sequencing
(8 pages, 2007)

110. E. Ivanov, O. Gluchshenko, H. Andrä, A. Kudryavtsev
Parallel software tool for decomposing and meshing of 3d structures
Keywords: a-priori domain decomposition, unstructured grid, Delaunay mesh generation
(14 pages, 2007)

111. O. Iliev, R. Lazarov, J. Willems
Numerical study of two-grid preconditioners for 1d elliptic problems with highly oscillating discontinuous coefficients
Keywords: two-grid algorithm, oscillating coefficients, preconditioner
(20 pages, 2007)

112. L. Bonilla, T. Götz, A. Klar, N. Marheineke, R. Wegener
Hydrodynamic limit of the Fokker-Planck-equation describing fiber lay-down processes
Keywords: stochastic dierential equations, Fokker-Planck equation, asymptotic expansion, Ornstein-Uhlenbeck process
(17 pages, 2007)

113. S. Rief
Modeling and simulation of the pressing section of a paper machine
Keywords: paper machine, computational fluid dynamics, porous media
(41 pages, 2007)

114. R. Ciegis, O. Iliev, Z. Lakdawala
On parallel numerical algorithms for simulating industrial filtration problems
Keywords: Navier-Stokes-Brinkmann equations, finite volume discretization method, SIMPLE, parallel computing, data decomposition method
(24 pages, 2007)

115. N. Marheineke, R. Wegener
Dynamics of curved viscous fibers with surface tension
Keywords: Slender body theory, curved viscous bers with surface tension, free boundary value problem
(25 pages, 2007)

116. S. Feth, J. Franke, M. Speckert
Resampling-Methoden zur mse-Korrektur und Anwendungen in der Betriebsfestigkeit
Keywords: Weibull, Bootstrap, Maximum-Likelihood, Betriebsfestigkeit
(16 pages, 2007)

117. H. Knaf
Kernel Fisher discriminant functions – a concise and rigorous introduction
Keywords: wild bootstrap test, texture classification, textile quality control, defect detection, kernel estimate, nonparametric regression
(30 pages, 2007)

118. O. Iliev, I. Rybak
On numerical upscaling for flows in heterogeneous porous media

Keywords: numerical upscaling, heterogeneous porous media, single phase flow, Darcy's law, multiscale problem, effective permeability, multipoint flux approximation, anisotropy
(17 pages, 2007)

119. O. Iliev, I. Rybak
On approximation property of multipoint flux approximation method
Keywords: Multipoint flux approximation, finite volume method, elliptic equation, discontinuous tensor coefficients, anisotropy
(15 pages, 2007)

120. O. Iliev, I. Rybak, J. Willems
On upscaling heat conductivity for a class of industrial problems
Keywords: Multiscale problems, effective heat conductivity, numerical upscaling, domain decomposition
(21 pages, 2007)

121. R. Ewing, O. Iliev, R. Lazarov, I. Rybak
On two-level preconditioners for flow in porous media
Keywords: Multiscale problem, Darcy's law, single phase flow, anisotropic heterogeneous porous media, numerical upscaling, multigrid, domain decomposition, efficient preconditioner
(18 pages, 2007)

122. M. Brickenstein, A. Dreyer
POLYBORI: A Gröbner basis framework for Boolean polynomials
Keywords: Gröbner basis, formal verification, Boolean polynomials, algebraic cryptoanalysis, satisfiability
(23 pages, 2007)

123. O. Wirjadi
Survey of 3d image segmentation methods
Keywords: image processing, 3d, image segmentation, binarization
(20 pages, 2007)

124. S. Zeytun, A. Gupta
A Comparative Study of the Vasicek and the CIR Model of the Short Rate
Keywords: interest rates, Vasicek model, CIR-model, calibration, parameter estimation
(17 pages, 2007)

125. G. Hanselmann, A. Sarishvili
Heterogeneous redundancy in software quality prediction using a hybrid Bayesian approach
Keywords: reliability prediction, fault prediction, non-homogeneous poisson process, Bayesian model averaging
(17 pages, 2007)

126. V. Maag, M. Berger, A. Winterfeld, K.-H. Küfer
A novel non-linear approach to minimal area rectangular packing
Keywords: rectangular packing, non-overlapping constraints, non-linear optimization, regularization, relaxation
(18 pages, 2007)

127. M. Monz, K.-H. Küfer, T. Bortfeld, C. Thieke
Pareto navigation – systematic multi-criteria-based IMRT treatment plan determination
Keywords: convex, interactive multi-objective optimization, intensity modulated radiotherapy planning
(15 pages, 2007)

128. M. Krause, A. Scherrer
On the role of modeling parameters in IMRT plan optimization
Keywords: intensity-modulated radiotherapy (IMRT), inverse IMRT planning, convex optimization, sensitivity analysis, elasticity, modeling parameters, equivalent uniform dose (EUD)
(18 pages, 2007)

129. A. Wiegmann
Computation of the permeability of porous materials from their microstructure by FFF-Stokes
Keywords: permeability, numerical homogenization, fast Stokes solver
(24 pages, 2007)

130. T. Melo, S. Nickel, F. Saldanha da Gama
Facility Location and Supply Chain Management – A comprehensive review
Keywords: facility location, supply chain management, network design
(54 pages, 2007)

131. T. Hanne, T. Melo, S. Nickel
Bringing robustness to patient flow management through optimized patient transports in hospitals
Keywords: Dial-a-Ride problem, online problem, case study, tabu search, hospital logistics
(23 pages, 2007)

132. R. Ewing, O. Iliev, R. Lazarov, I. Rybak, J. Willems
An efficient approach for upscaling properties of composite materials with high contrast of coefficients
Keywords: effective heat conductivity, permeability of fractured porous media, numerical upscaling, fibrous insulation materials, metal foams
(16 pages, 2008)

133. S. Gelareh, S. Nickel
New approaches to hub location problems in public transport planning
Keywords: integer programming, hub location, transportation, decomposition, heuristic
(25 pages, 2008)

134. G. Thömmes, J. Becker, M. Junk, A. K. Vaikuntam, D. Kehrwald, A. Klar, K. Steiner, A. Wiegmann
A Lattice Boltzmann Method for immiscible multiphase flow simulations using the Level Set Method
Keywords: Lattice Boltzmann method, Level Set method, free surface, multiphase flow
(28 pages, 2008)

135. J. Orlik
Homogenization in elasto-plasticity
Keywords: multiscale structures, asymptotic homogenization, nonlinear energy
(40 pages, 2008)

136. J. Almquist, H. Schmidt, P. Lang, J. Deitmer, M. Jirstrand, D. Prätzel-Wolters, H. Becker
Determination of interaction between MCT1 and CAII via a mathematical and physiological approach
Keywords: mathematical modeling; model reduction; electrophysiology; pH-sensitive microelectrodes; proton antenna
(20 pages, 2008)

137. E. Savenkov, H. Andrä, O. Iliev
An analysis of one regularization approach for solution of pure Neumann problem
Keywords: pure Neumann problem, elasticity, regularization, finite element method, condition number
(27 pages, 2008)

138. O. Berman, J. Kalcsics, D. Krass, S. Nickel
The ordered gradual covering location problem on a network
Keywords: gradual covering, ordered median function, network location
(32 pages, 2008)

139. S. Gelareh, S. Nickel
Multi-period public transport design: A novel model and solution approaches
Keywords: Integer programming, hub location, public transport, multi-period planning, heuristics
(31 pages, 2008)

140. T. Melo, S. Nickel, F. Saldanha-da-Gama
Network design decisions in supply chain planning
Keywords: supply chain design, integer programming models, location models, heuristics
(20 pages, 2008)

141. C. Lautensack, A. Särkkä, J. Freitag, K. Schladitz
Anisotropy analysis of pressed point processes
Keywords: estimation of compression, isotropy test, nearest neighbour distance, orientation analysis, polar ice, Ripley's K function
(35 pages, 2008)

142. O. Iliev, R. Lazarov, J. Willems
A Graph-Laplacian approach for calculating the effective thermal conductivity of complicated fiber geometries
Keywords: graph laplacian, effective heat conductivity, numerical upscaling, fibrous materials
(14 pages, 2008)

143. J. Linn, T. Stephan, J. Carlsson, R. Bohlin
Fast simulation of quasistatic rod deformations for VR applications
Keywords: quasistatic deformations, geometrically exact rod models, variational formulation, energy minimization, finite differences, nonlinear conjugate gradients
(7 pages, 2008)

144. J. Linn, T. Stephan
Simulation of quasistatic deformations using discrete rod models
Keywords: quasistatic deformations, geometrically exact rod models, variational formulation, energy minimization, finite differences, nonlinear conjugate gradients
(9 pages, 2008)

145. J. Marburger, N. Marheineke, R. Pinnau
Adjoint based optimal control using mesh-less discretizations
Keywords: Mesh-less methods, particle methods, Eulerian-Lagrangian formulation, optimization strategies, adjoint method, hyperbolic equations
(14 pages, 2008

146. S. Desmettre, J. Gould, A. Szimayer
Own-company stockholding and work effort preferences of an unconstrained executive
Keywords: optimal portfolio choice, executive compensation
(33 pages, 2008)

147. M. Berger, M. Schröder, K.-H. Küfer
A constraint programming approach for the two-dimensional rectangular packing problem with orthogonal orientations
Keywords: rectangular packing, orthogonal orientations non-overlapping constraints, constraint propagation
(13 pages, 2008)

148. K. Schladitz, C. Redenbach, T. Sych, M. Godehardt
Microstructural characterisation of open foams using 3d images
Keywords: virtual material design, image analysis, open foams
(30 pages, 2008)

149. E. Fernández, J. Kalcsics, S. Nickel, R. Ríos-Mercado
A novel territory design model arising in the implementation of the WEEE-Directive
Keywords: heuristics, optimization, logistics, recycling
(28 pages, 2008)

150. H. Lang, J. Linn
Lagrangian field theory in space-time for geometrically exact Cosserat rods
Keywords: Cosserat rods, geometrically exact rods, small strain, large deformation, deformable bodies, Lagrangian field theory, variational calculus
(19 pages, 2009)

151. K. Dreßler, M. Speckert, R. Müller, Ch. Weber
Customer loads correlation in truck engineering
Keywords: Customer distribution, safety critical components, quantile estimation, Monte-Carlo methods
(11 pages, 2009)

152. H. Lang, K. Dreßler
An improved multiaxial stress-strain correction model for elastic FE postprocessing
Keywords: Jiang's model of elastoplasticity, stress-strain correction, parameter identification, automatic differentiation, least-squares optimization, Coleman-Li algorithm
(6 pages, 2009)

153. J. Kalcsics, S. Nickel, M. Schröder
A generic geometric approach to territory design and districting
Keywords: Territory design, districting, combinatorial optimization, heuristics, computational geometry
(32 pages, 2009)

154. Th. Fütterer, A. Klar, R. Wegener
An energy conserving numerical scheme for the dynamics of hyperelastic rods
Keywords: Cosserat rod, hyperealstic, energy conservation, finite differences
(16 pages, 2009)

155. A. Wiegmann, L. Cheng, E. Glatt, O. Iliev, S. Rief
Design of pleated filters by computer simulations
Keywords: Solid-gas separation, solid-liquid separation, pleated filter, design, simulation
(21 pages, 2009)

156. A. Klar, N. Marheineke, R. Wegener
Hierarchy of mathematical models for production processes of technical textiles
Keywords: Fiber-fluid interaction, slender-body theory, turbulence modeling, model reduction, stochastic differential equations, Fokker-Planck equation, asymptotic expansions, parameter identification
(21 pages, 2009)

157. E. Glatt, S. Rief, A. Wiegmann, M. Knefel, E. Wegenke
Structure and pressure drop of real and virtual metal wire meshes
Keywords: metal wire mesh, structure simulation, model calibration, CFD simulation, pressure loss
(7 pages, 2009)

158. S. Kruse, M. Müller
Pricing American call options under the assumption of stochastic dividends – An application of the Korn-Rogers model
Keywords: option pricing, American options, dividends, dividend discount model, Black-Scholes model
(22 pages, 2009)

159. H. Lang, J. Linn, M. Arnold
Multibody dynamics simulation of geometrically exact Cosserat rods
Keywords: flexible multibody dynamics, large deformations, finite rotations, constrained mechanical systems, structural dynamics
(20 pages, 2009)

160. P. Jung, S. Leyendecker, J. Linn, M. Ortiz
Discrete Lagrangian mechanics and geometrically exact Cosserat rods
Keywords: special Cosserat rods, Lagrangian mechanics, Noether's theorem, discrete mechanics, frame-indifference, holonomic constraints
(14 pages, 2009)

161. M. Burger, K. Dreßler, A. Marquardt, M. Speckert
Calculating invariant loads for system simulation in vehicle engineering
Keywords: iterative learning control, optimal control theory, differential algebraic equations (DAEs)
(18 pages, 2009)

162. M. Speckert, N. Ruf, K. Dreßler
Undesired drift of multibody models excited by measured accelerations or forces
Keywords: multibody simulation, full vehicle model, force-based simulation, drift due to noise
(19 pages, 2009)

163. A. Streit, K. Dreßler, M. Speckert, J. Lichter, T. Zenner, P. Bach
Anwendung statistischer Methoden zur Erstellung von Nutzungsprofilen für die Auslegung von Mobilbaggern
Keywords: Nutzungsvielfalt, Kundenbeanspruchung, Bemessungsgrundlagen
(13 pages, 2009)

164. I. Correia, S. Nickel, F. Saldanha-da-Gama
The capacitated single-allocation hub location problem revisited: A note on a classical formulation
Keywords: Capacitated Hub Location, MIP formulations
(10 pages, 2009)

165. F. Yaneva, T. Grebe, A. Scherrer
An alternative view on global radiotherapy optimization problems
Keywords: radiotherapy planning, path-connected sublevelsets, modified gradient projection method, improving and feasible directions
(14 pages, 2009)

166. J. I. Serna, M. Monz, K.-H. Küfer, C. Thieke
Trade-off bounds and their effect in multi-criteria IMRT planning
Keywords: trade-off bounds, multi-criteria optimization, IMRT, Pareto surface
(15 pages, 2009)

167. W. Arne, N. Marheineke, A. Meister, R. Wegener
Numerical analysis of Cosserat rod and string models for viscous jets in rotational spinning processes
Keywords: Rotational spinning process, curved viscous fibers, asymptotic Cosserat models, boundary value problem, existence of numerical solutions
(18 pages, 2009)

168. T. Melo, S. Nickel, F. Saldanha-da-Gama
An LP-rounding heuristic to solve a multi-period facility relocation problem
Keywords: supply chain design, heuristic, linear programming, rounding
(37 pages, 2009)

169. I. Correia, S. Nickel, F. Saldanha-da-Gama
Single-allocation hub location problems with capacity choices
Keywords: hub location, capacity decisions, MILP formulations
(27 pages, 2009)

170. S. Acar, K. Natcheva-Acar
A guide on the implementation of the Heath-Jarrow-Morton Two-Factor Gaussian Short Rate Model (HJM-G2++)
Keywords: short rate model, two factor Gaussian, G2++, option pricing, calibration
(30 pages, 2009)

171. A. Szimayer, G. Dimitroff, S. Lorenz
A parsimonious multi-asset Heston model: calibration and derivative pricing
Keywords: Heston model, multi-asset, option pricing, calibration, correlation
(28 pages, 2009)

172. N. Marheineke, R. Wegener
Modeling and validation of a stochastic drag for fibers in turbulent flows
Keywords: fiber-fluid interactions, long slender fibers, turbulence modelling, aerodynamic drag, dimensional analysis, data interpolation, stochastic partial differential algebraic equation, numerical simulations, experimental validations
(19 pages, 2009)

173. S. Nickel, M. Schröder, J. Steeg
Planning for home health care services
Keywords: home health care, route planning, metaheuristics, constraint programming
(23 pages, 2009)

174. G. Dimitroff, A. Szimayer, A. Wagner
Quanto option pricing in the parsimonious Heston model
Keywords: Heston model, multi asset, quanto options, option pricing
(14 pages, 2009) 174. G. Dimitroff, A. Szimayer, A. Wagner

175. S. Herkt, K. Dreßler, R. Pinnau
Model reduction of nonlinear problems in structural mechanics
Keywords: flexible bodies, FEM, nonlinear model reduction, POD
(13 pages, 2009)

176. M. K. Ahmad, S. Didas, J. Iqbal
Using the Sharp Operator for edge detection and nonlinear diffusion
Keywords: maximal function, sharp function,image processing, edge detection, nonlinear diffusion
(17 pages, 2009)

177. M. Speckert, N. Ruf, K. Dreßler, R. Müller, C. Weber, S. Weihe
Ein neuer Ansatz zur Ermittlung von Erprobungslasten für sicherheitsrelevante Bauteile
Keywords: sicherheitsrelevante Bauteile, Kundenbeanspruchung, Festigkeitsverteilung, Ausfallwahrscheinlichkeit, Konfidenz, statistische Unsicherheit, Sicherheitsfaktoren
(16 pages, 2009)

178. J. Jegorovs
Wave based method: new applicability areas
Keywords: Elliptic boundary value problems, inhomogeneous Helmholtz type differential equations in bounded domains, numerical methods, wave based method, uniform B-splines
(10 pages, 2009)

179. H. Lang, M. Arnold
Numerical aspects in the dynamic simulation of geometrically exact rods
Keywords: Kirchhoff and Cosserat rods, geometrically exact rods, deformable bodies, multibody dynamics,artial differential algebraic equations, method of lines, time integration
(21 pages, 2009)

180. H. Lang
Comparison of quaternionic and rotation-free null space formalisms for multibody dynamics
Keywords: Parametrisation of rotations, differential-algebraic equations, multibody dynamics, constrained mechanical systems, Lagrangian mechanics
(40 pages, 2010)

181. S. Nickel, F. Saldanha-da-Gama, H.-P. Ziegler
Stochastic programming approaches for risk aware supply chain network design problems
Keywords: Supply Chain Management, multi-stage stochastic programming, financial decisions, risk
(37 pages, 2010)

182. P. Ruckdeschel, N. Horbenko
Robustness properties of estimators in generalized Pareto Models
Keywords: global robustness, local robustness, finite sample breakdown point, generalized Pareto distribution
(58 pages, 2010)

183. P. Jung, S. Leyendecker, J. Linn, M. Ortiz
A discrete mechanics approach to Cosserat rod theory – Part 1: static equilibria
Keywords: Special Cosserat rods; Lagrangian mechanics; Noether's theorem; discrete mechanics; frame-indifference; holonomic constraints; variational formulation
(35 pages, 2010)

184. R. Eymard, G. Printsypar
A proof of convergence of a finite volume scheme for modified steady Richards' equation describing transport processes in the pressing section of a paper machine
Keywords: flow in porous media, steady Richards' equation, finite volume methods, convergence of approximate solution
(14 pages, 2010)

185. P. Ruckdeschel
Optimally Robust Kalman Filtering
Keywords: robustness, Kalman Filter, innovation outlier, additive outlier
(42 pages, 2010)

186. S. Repke, N. Marheineke, R. Pinnau
On adjoint-based optimization of a free surface Stokes flow
Keywords: film casting process, thin films, free surface Stokes flow, optimal control, Lagrange formalism
(13 pages, 2010)

187. O. Iliev, R. Lazarov, J. Willems
Variational multiscale Finite Element Method for flows in highly porous media
Keywords: numerical upscaling, flow in heterogeneous porous media, Brinkman equations, Darcy's law, subgrid approximation, discontinuous Galerkin mixed FEM
(21 pages, 2010)

188. S. Desmettre, A. Szimayer
Work effort, consumption, and portfolio selection: When the occupational choice matters
Keywords: portfolio choice, work effort, consumption, occupational choice
(34 pages, 2010)

189. O. Iliev, Z. Lakdawala, V. Starikovicius
On a numerical subgrid upscaling algorithm for Stokes-Brinkman equations
Keywords: Stokes-Brinkman equations, subgrid approach, multiscale problems, numerical upscaling
(27 pages, 2010)

190. A. Latz, J. Zausch, O. Iliev
Modeling of species and charge transport in Li-Ion Batteries based on non-equilibrium thermodynamics
Keywords: lithium-ion battery, battery modeling, electrochemical simulation, concentrated electrolyte, ion transport
(8 pages, 2010)

191. P. Popov, Y. Vutov, S. Margenov, O. Iliev
Finite volume discretization of equations describing nonlinear diffusion in Li-Ion batteries
Keywords: nonlinear diffusion, finite volume discretization, Newton method, Li-Ion batteries
(9 pages, 2010)

192. W. Arne, N. Marheineke, R. Wegener
Asymptotic transition from Cosserat rod to string models for curved viscous inertial jets
Keywords: rotational spinning processes; inertial and viscous-inertial fiber regimes; asymptotic limits; slender-body theory; boundary value problems
(23 pages, 2010)

193. L. Engelhardt, M. Burger, G. Bitsch
Real-time simulation of multibody-systems for on-board applications
Keywords: multibody system simulation, real-time simulation, on-board simulation, Rosenbrock methods
(10 pages, 2010)

194. M. Burger, M. Speckert, K. Dreßler
Optimal control methods for the calculation of invariant excitation signals for multibody systems
Keywords: optimal control, optimization, mbs simulation, invariant excitation
(9 pages, 2010)

195. A. Latz, J. Zausch
Thermodynamic consistent transport theory of Li-Ion batteries
Keywords: Li-Ion batteries, nonequilibrium thermodynamics, thermal transport, modeling
(18 pages, 2010)

196. S. Desmettre
Optimal investment for executive stockholders with exponential utility
Keywords: portfolio choice, executive stockholder, work effort, exponential utility
(24 pages, 2010)

197. W. Arne, N. Marheineke, J. Schnebele, R. Wegener
Fluid-fiber-interactions in rotational spinning process of glass wool production
Keywords: Rotational spinning process, viscous thermal jets, fluid-fiber-interactions, two-way coupling, slender-body theory, Cosserat rods, drag models, boundary value problem, continuation method
(20 pages, 2010)

Status quo: December 2010